Cancer Biol Med 2025. doi: 10.20892/j.issn.2095-3941.2024.0514

ORIGINAL ARTICLE

Comprehensive strategies for management of postoperative hyper-progression recurrence (HPR) of hepatocellular carcinoma: a 12-year large sample multi-center study

Lunan Qi[1,2,3]*, Jingxuan Xu[1,3]*, Yuanyuan Chen[3,4], Zhan Lu[1,3,5], Min Zhou[3,6], Yingwu Huang[7], Yongchi Ling[8], Hai Huang[9], Yuchong Peng[10], Tao Peng[2,3,11], Bangde Xiang[1,2,3], Liang Ma[1,2,3]

[1]Department of Hepatobiliary Surgery, Guangxi Medical University Cancer Hospital, Nanning 530021, China; [2]Guangxi Liver Cancer Diagnosis and Treatment Engineering and Technology Research Center, Nanning 530021, China; [3]Key Laboratory of Early Prevention and Treatment for Regional High Frequency Tumor, Ministry of Education, Nanning 530021, China; [4]Department of Ultrasound, First Affiliated Hospital of Guangxi Medical University, Nanning 530021, China; [5]Department of Hepatobiliary Surgery, Guangxi International Zhuang Medical Hospital, Nanning 530021, China; [6]Department of General Surgery, Liuzhou Workers' Hospital, Liuzhou 545005, China; [7]Department of Hepatobiliary Surgery, Chongzuo People's Hospital, Chongzuo 532200, China; [8]Department of Surgery, Fusui County People's Hospital of Guangxi, Fusui 543200, China; [9]Department of Hepatobiliary Surgery, Wuming Hospital of Guangxi Medical University, Wuming 530100, China; [10]Department of General Surgery, Chongqing Hospital of Traditional Chinese Medicine, Chongqing 400021, China; [11]Department of Hepatobiliary Surgery, First Affiliated Hospital of Guangxi Medical University, Nanning 530021, China

ABSTRACT

Objective: Hyper-progression recurrence (HPR) after hepatectomy is a specific recurrence pattern associated with extremely poor prognosis in patients with hepatocellular carcinoma (HCC). This study was aimed at investigating the probable risk factors and establishing comprehensive models for formulating clinical strategies.

Methods: Overall, 16,158 patients with HCC from 8 hospitals were screened, among whom 3,125 patients who underwent R0 resection were included, and divided into development (n = 2,113) and validation (n = 1,012) cohorts. A comprehensive study of HPR predictive models and biological features was conducted.

Results: Among the 3,125 enrolled patients, 506 (16.19%) developed HPR. The influence of HPR on extremely poor prognosis was reflected by recurrence features, adverse effects on systemic and liver function, and limited therapeutic options. Nine variables closely associated with HPR were identified, and incorporated into nomogram and conditional inference tree models, which successfully achieved pre- and post-operative HPR risk stratification and facilitated clinical decision-making. Multi-dimensional verification also confirmed the predictive accuracy of model combinations and their reliability in clinical applications. Furthermore, biological analyses revealed that HCCs with HPR exhibited hyperactive biological processes, inactive metabolism, and immune exhaustion features, together with high MYCN/HMGA2 co-expression, thereby enhancing understanding of the molecular events leading to HPR and providing valuable knowledge for HPR management.

Conclusions: HPR after hepatectomy is associated with extremely poor prognosis and requires substantial attention. We constructed comprehensive predictive models and propose a clinical strategy for guiding HPR prevention and management.

KEYWORDS Hepatocellular carcinoma; hyper-progression recurrence; predictive models; biological feature; clinical strategy

*These authors contributed equally to this work.
Correspondence to: Lunan Qi and Liang Ma
E-mail: qilunan_gxmu@163.com, wangzhennuo@aliyun.com and malianggxyd@163.com
ORCID ID: https://orcid.org/0000-0003-0254-6982 and https://orcid.org/0000-0001-8106-373X
Received November 14, 2024; accepted April 15, 2025;
published online July 11, 2025.
Available at www.cancerbiomed.org
©2025 The Authors. Creative Commons Attribution-NonCommercial 4.0 International License

Introduction

Hepatocellular carcinoma (HCC) is the third leading cause of cancer-related death worldwide[1]. With improvements in surgical techniques and perioperative management of patients, HCC can be resected safely. However, the high incidence of post-surgical recurrence severely compromises long-term survival[2,3]. Therefore, the effective control of post-surgical recurrence to increase the overall efficacy of HCC has

become an important area of focus in the era of precision medicine.

Meaningful survival can be achieved with appropriate prevention and treatment of recurrence[2]. Various therapeutics have been used to manage recurrence, including adjuvant therapeutics for recurrence prevention and anti-recurrence therapeutics[4-12]. However, varied outcomes have been observed in patients undergoing active anti-recurrence treatment, primarily because of the multiplicity of recurrence patterns. In our previous study, we proposed a novel four-type classification for recurrent HCC with potential value for predicting survival and guiding treatment strategies[13]. Notably, type IV recurrence, also called hyper-progression recurrence (HPR), involves the sudden simultaneous occurrence of multiple intrahepatic recurrence nodules (>5 recurrence lesions) in the early postoperative period[13]. Patients experiencing HPR have extremely poor prognosis, owing to rapid deterioration. Furthermore, HPR may occur in patients with different HCC stages, including early stage. Therefore, improving understanding of the implications of HPR and developing prevention strategies are crucial. However, our previous research has not extensively explored HPR risk factors and preventive strategies. In addition, to our knowledge, no prior report has focused on HPR.

Given that HPR can occur in patients with various HCC stages, the commonly used staging systems have limited value in HPR prediction. Therefore, we conducted a large sample study of multicenter cohorts to further investigate HPR risk factors. Subsequently, we established a nomogram and conditional inference tree (CTREE) models based on the identified risk factors to comprehensively assess HPR risk. Furthermore, we used a "model layer pass" approach and combined the biological features of HPR to develop a clinical strategy to guide HPR prevention and management.

Materials and methods

Patients and follow-up

From January 2010 to March 2021, 16,158 patients with HCC at 8 hospitals (Guangxi Medical University Cancer Hospital, First Affiliated Hospital of Guangxi Medical University, Liuzhou Workers' Hospital, Chongzuo People's Hospital, Chongqing Hospital of Traditional Chinese Medicine, Wuming Hospital of Guangxi Medical University, Fusui County People's Hospital, and Guangxi International Zhuang Medical Hospital) were screened. Finally, 3,125 patients who underwent R0 resection (according to the intraoperative criteria in the Guidelines for the Diagnosis and Treatment of Primary Liver Cancer[14]) with a mean age of 45 years (range: 14–83 years) were enrolled. The inclusion criteria were as follows: 1) treatment with R0 resection; 2) definitive pathological diagnosis of HCC according to World Health Organization criteria; 3) no prior anticancer treatment; and 4) tumor stage determined according to the Chinese Liver Cancer staging system[14] and tumor differentiation defined according to the Edmondson grading system. The baseline data and follow-up of each center are shown in **Table S1**.

HPR was defined as the first sudden simultaneous appearance of numerous intrahepatic nodules (>5) without (type A) or with (type B) macrovascular invasion or extra-hepatic metastasis in the early postoperative period (within 2 years)[13]. According to the above definition, all patients included in this study were required to have either definite recurrence or regular follow-up over 2 years, to better identify patients with HPR. Therefore, patients with less than 2 years of follow-up and no definite recurrence at their last assessment were excluded. The end-point of the follow-up was January 31, 2023. Cohort information and the study design are shown in the supplementary information and **Figure 1A**.

Ethics statement

The ethics committee of each participating center approved this study's protocol (approval No. LW2018034). Written informed consent was obtained from the patients. All procedures were performed according to the ethical standards of the Helsinki Declaration of 1975, revised in 1983.

Supplementary information

The supplementary information provides detailed information, including patients and follow-up, clinicopathological factors, RNA-seq analysis, data acquisition, immunohistochemical staining, real-time quantitative PCR, and supplementary figures.

Statistical analysis

All statistical analyses were performed in IBM SPSS statistical software version 22 for Windows and R version 3.6.1 (IBM, Armonk, NY, USA). The clinicopathological characteristics of the development and validation cohorts were evaluated with χ^2 test or Fisher's exact test. In addition, overall survival (OS)

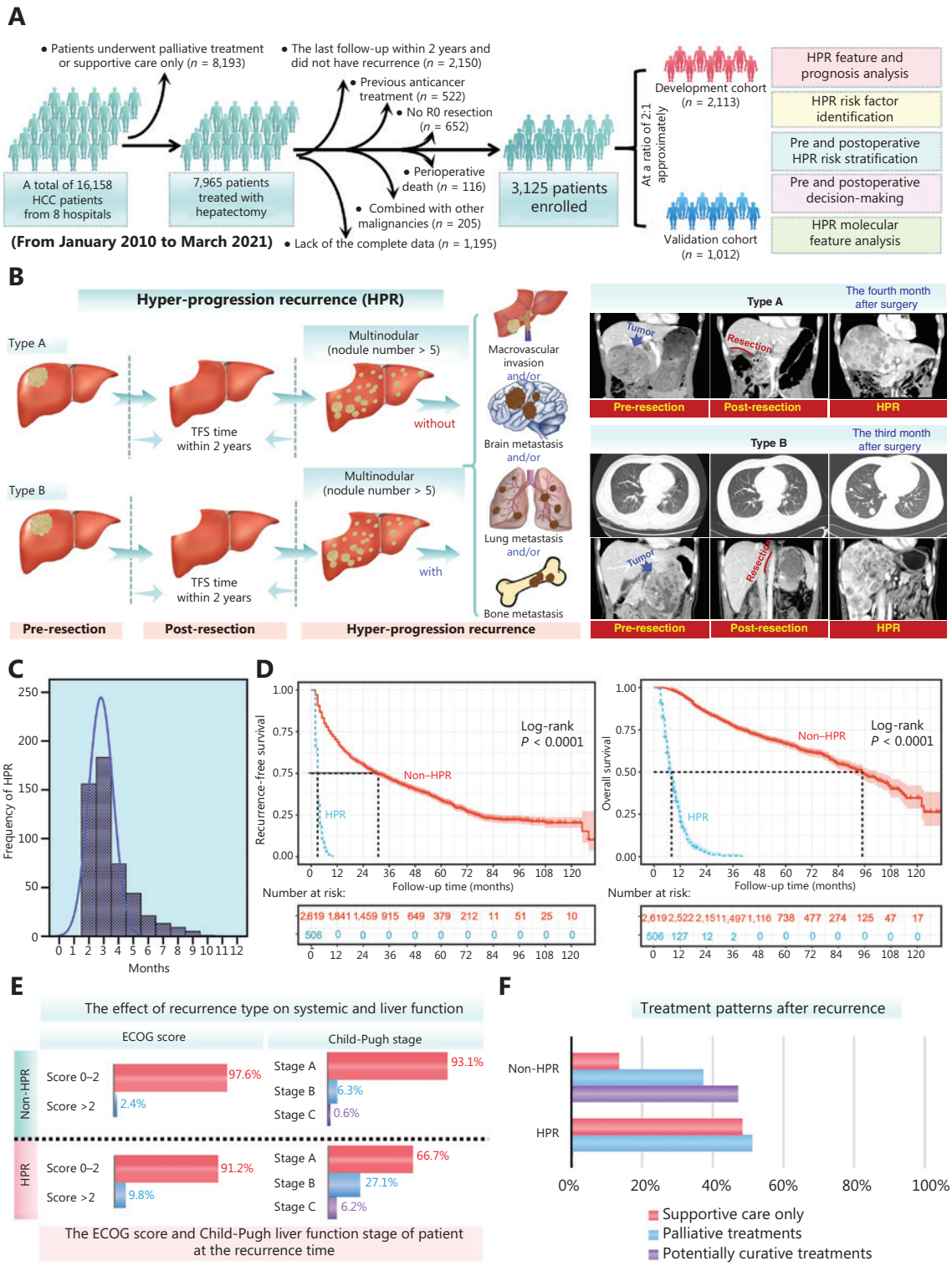
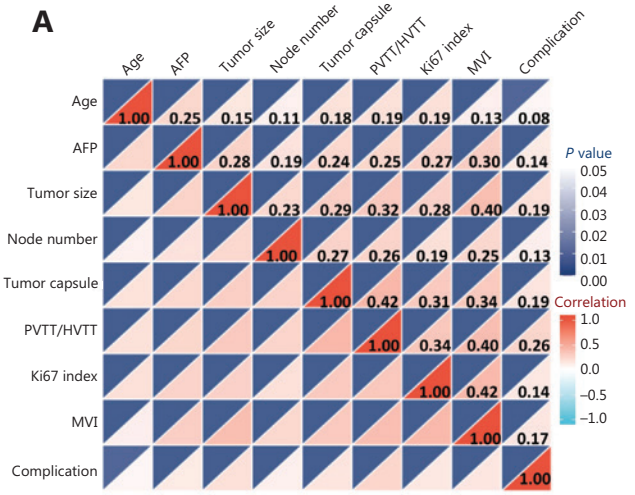


Figure 1 Characteristics of HPR and influence on patient prognosis. (A) Flow chart of patient enrollment. (B) Representative pattern diagram and image of two types of HPR. (C) Graph of HPR occurrence times. (D) Comparison of RFS and OS between patients with HPR after hepatectomy and patients without HPR. (E) ECOG score and Child-Pugh liver function stage in patients during HPR. (F) Comparison of post-recurrence treatment modalities between patients with *vs.* without HPR.

Table 1 Univariate and multivariate logistic analysis of patients' clinicopathologic characteristics associated with HPR

Characteristics		Univariate		Multivariate	
		OR (95% CI)	*P*	OR (95% CI)	*P*
Age	≤ 45 years *vs*. > 45 years	5.231 (3.994, 6.851)	<0.001*	4.956 (3.209, 7.656)	<0.001*
Sex	Male *vs*. female	0.862 (0.593, 1.293)	0.436		
HBsAg	Positive *vs*. negative	0.980 (0.672, 1.430)	0.591		
HCV (anti-HCV)	Positive *vs*. negative	1.387 (0.921, 2.093)	0.122		
HBV-DNA	≥ 500 *vs*. < 500 IU/mL	1.414 (1.079, 1.851)	0.012*	0.787 (0.500, 1.238)	0.299
Serum AFP level	≥ 400 *vs*. < 400 ng/mL	5.805 (4.338, 7.767)	<0.001*	1.770 (1.137, 2.755)	0.011*
Smoking	Yes *vs*. no	1.154 (0.905–1.471)	0.262		
Alcoholism	Yes *vs*. no	1.227 (0.789–1.884)	0.381		
Comorbid illnesses	Presence *vs*. absence	0.566 (0.316, 0.921)	0.137		
Liver fibrosis (Fib-4 score)	≤ 3.25 *vs*. > 3.25	0.655 (0.486, 0.884)	0.006*	0.769 (0.469, 1.261)	0.298
Child-Pugh score	Stage A *vs*. stage B	0.712 (0.235, 2.157)	0.548		
Tumor size▲	5–10 *vs*. < 5 cm	8.189 (4.086, 16.41)	<0·001*	1.948 (1.735, 9.197)	0.120
	>10 cm *vs*. < 5 cm	38.12 (19.29, 75.34)	<0.001*	3.995 (2.389, 6.706)	0.001*
Edmondson grade▲	Poorly *vs*. well differentiated	1.697 (1.296, 2.220)	<0.001*	4.804 (0.471, 49.03)	0.186
Node number	2–3 nodes *vs*. single	1.135 (0.725, 1.778)	0.579	1.776 (0.963, 3.275)	0.066
	>3 nodes *vs*. single	14.58 (10.73, 19.81)	<0.001*	6.974 (4.281, 11.36)	<0.001*
Resection margin	>1 cm *vs*. ≤ 1 cm	1.203 (0.922, 1.570)	0.172		
MVD	High *vs*. low	0.972 (0.756, 1.251)	0·828		
MVI	Positive *vs*. negative	27.26 (15.17, 48.96)	<0.001*	2.720 (1.274, 5.810)	0.010*
PVTT/HVTT	Positive *vs*. negative	20.73 (15.35, 28.01)	<0.001*	4.128 (2.659, 6.410)	<0.001*
Tumor capsule▲	Incomplete *vs*. complete	11.66 (8.787, 15.47)	<0.001*	2.543 (1.663, 3.889)	<0.001*
Ki67 index (%)	30%–59% *vs*. ≤ 29%	8.486 (4.439, 16.22)	<0.001*	4.198 (1.968, 8.875)	<0.001*
	≥60% *vs*. ≤ 29%	68.56 (36.78, 127.79)	<0.001*	23.18 (11.07, 48.53)	<0.001*
Intraoperative blood loss	≤500 mL *vs*. > 500 mL	0.789 (0.602–1.031)	0.191		
Post-operative complications (Clavien-Dindo ≥ grade II)	Presence *vs*. absence	8.759 (6.287, 12.21)	<0.001*	6.879 (3.827, 12.36)	<0.001*
Ideal BMI		0.985 (0.931, 1.201)	0.207		

OR, odds ratio; CI, confidence intervals; HCV, hepatitis C virus; AFP, alpha-fetoprotein; MVI, microvascular invasion; PVTT, portal vein tumor thrombus; MVD, microvascular density.
▲If the patient had multiple nodes, the largest one was recorded. *$P < 0.05$.



B

Variable	VIF	Tolerance
Age	1.0969	0.9124
AFP	1.2098	0.8265
Tumor size	1.3123	0.7621
Node number	1.1978	0.8348
Tumor capsule	1.3575	0.7366
PVTT/HVTT	1.4495	0.6898
Ki67 index	1.3321	0.7507
MVI	1.4463	0.6914
Complication	1.0871	0.9198
Mean	1.2765	0.7915

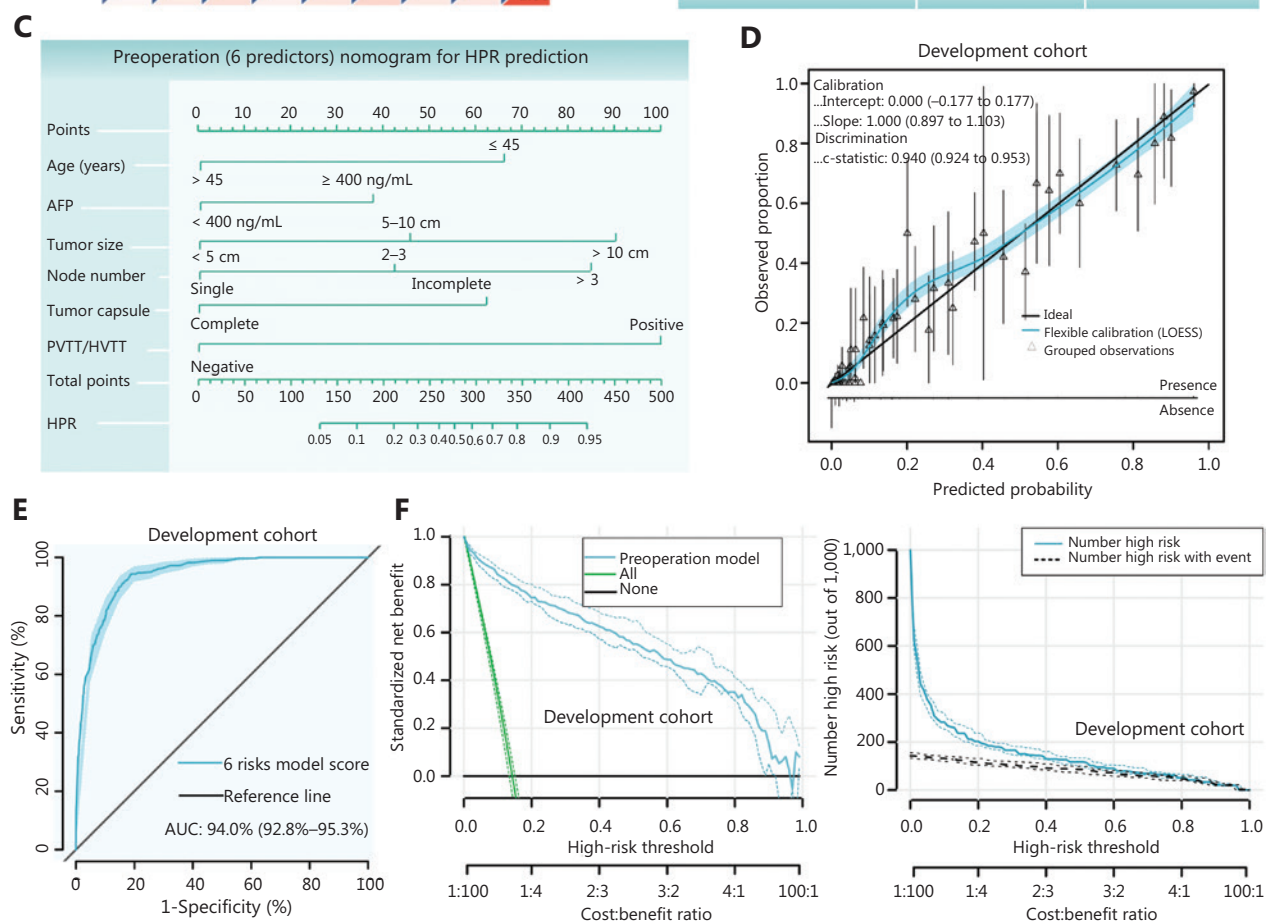


Figure 2 Identification of HPR predictors, establishment of a preoperative nomogram prediction model, and predictive performance evaluation. (A) The nine variables were analyzed with univariate and multivariate analyses, and the coefficient between each variable. (B) Multicollinearity analysis of the variance inflation factor for each variable. (C) Preoperative nomogram model for HPR prediction based on six preoperative predictors. (D) Calibration plots for the preoperative nomogram model in the development cohort. (E) ROC curve analyses indicating good HPR predictive performance of the preoperative nomogram model in the development cohort. (F) DCA and clinical impact curves of the preoperative nomogram model for predicting HPR in the development cohort.

and recurrence-free survival (RFS) were estimated with the Kaplan-Meier method and compared between groups with the log-rank test. Univariate and multivariate logistic regression analyses were conducted to identify independent predictors based on variables in the development cohort. In the univariate logistic regression analysis, potential predictors ($P < 0.05$) were further included in subsequent multivariate regression analysis (using the forward likelihood ratio method, with $P < 0.05$ as the entry and removal criteria).

Nomogram models were established according to the results of multivariable logistic regression analysis. The "rms" package in R was used to develop the nomograms. In the nomogram, "points" represents the score of each variable under different values, whereas "total points" represent the sum of the individual term points for all variables included in the model. Concordance statistics was used to measure the discriminative ability of the nomogram, and a calibration plot was drawn to reflect the agreement between the observed outcomes and predicted probabilities. Each patient's score on the nomogram was computed. Receiver operating characteristic (ROC) curve analysis was applied to further evaluate the predictive performance of the nomogram score and identify the optimal cut-off based on the maximal Youden index. The clinical utility of the nomogram was determined through decision curve analysis (DCA) after calculation of the net benefits at each risk threshold probability. The clinical impact curve of the nomogram was also plotted to demonstrate the significance of the nomogram.

A CTREE model was used for HPR risk stratification. The CTREE determines the optimal split of a parent node (a region in the feature space) with multiple testing procedures at each stage. According to the Gini criteria, patients were partitioned into 2 child nodes from the entire feature space, and risk tree growth and pruning continued until the terminal nodes had no subsequent splits attaining statistical significance. The probability of HPR was calculated for each terminal node and accordingly yielded a risk stratification model. All statistical assessments were two-tailed, and the threshold for statistical significance was set at $P < 0.05$.

Results

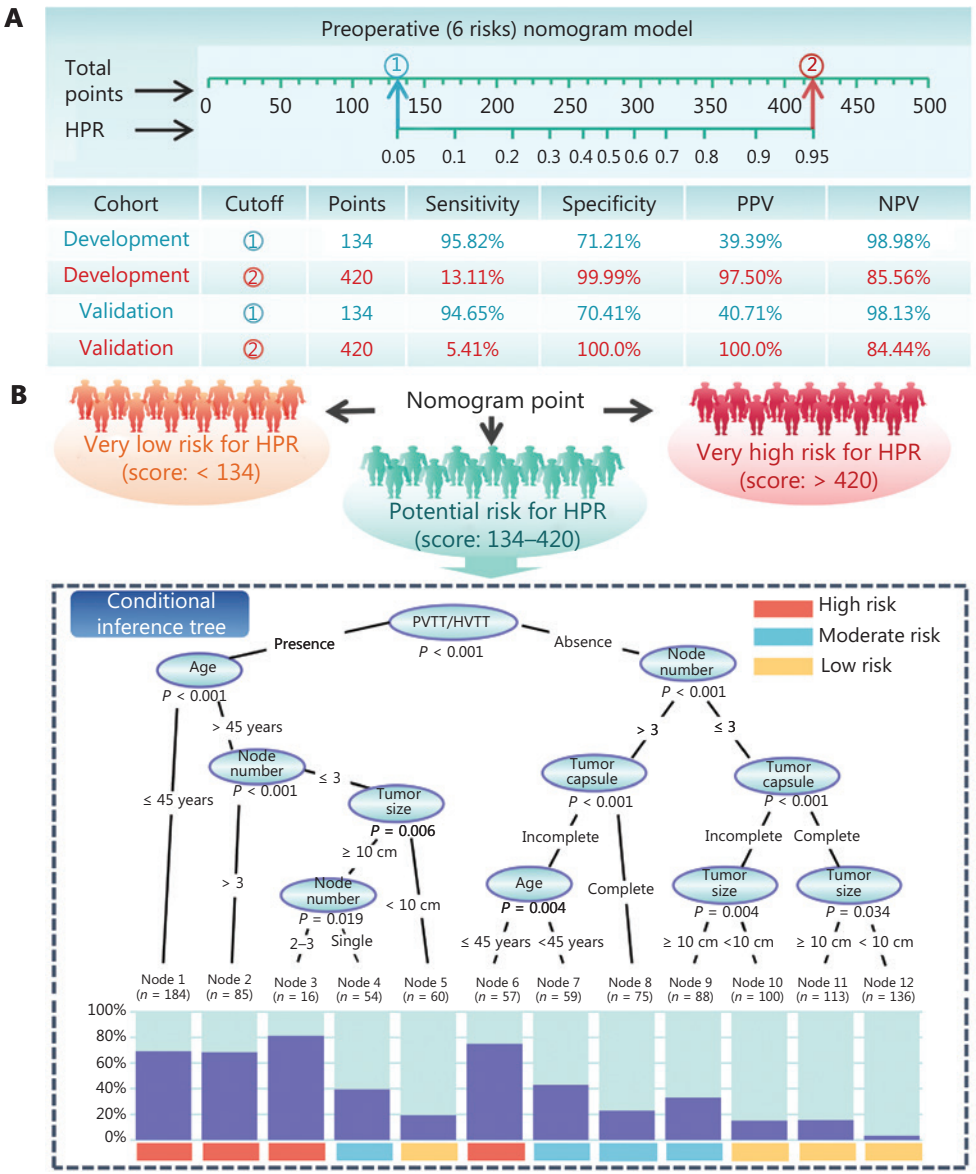
Characteristics and prognosis of HPR

In this multi-center study, HPR was observed in 16.19% (506/3,125) of patients: 233 and 273 with types A and B, respectively (**Figure 1B**). Analysis of the time to recurrence (TTR) of HPR confirmed that all HPR occurred in the early postoperative period (within 2 years), and the high incidence period was 2–4 months after hepatectomy (**Figure 1C**). The log-rank test indicated that patients with HPR (either type A or B) after hepatectomy had significantly lower RFS and OS than those without HPR (all $P < 0.05$) (**Figure 1D**).

During the study, 2,165 of the 3,125 patients experienced recurrence. The effects on systemic and liver function during recurrence and treatment after recurrence were analyzed in 2,165 patients with definite recurrence. Higher proportions of patients with poor Eastern Cooperative Oncology Group (ECOG) scores (>2) and poor liver function (stage B or C) were observed in patients with HPR during recurrence than those without HPR (**Figure 1E**). In addition, more than half the patients without HPR (57.3%) underwent curative treatment, including re-resection, liver transplantation, local ablation, or combined potentially curative treatment. In contrast, all patients with HPR received palliative treatments [e.g., transcatheter arterial chemoembolization (TACE)/hepatic artery infusion chemotherapy (HAIC), radiotherapy, or systemic treatment] or supportive care (e.g., Chinese medicine, treatment of liver function, symptomatic treatment, and/or nutritional support) alone (**Figure 1F**).

Risk factors for HPR identification

Subsequently, we explored the risk factors for HPR. First, the 3,125 patients were randomly divided into development (n = 2,113) and validation (n = 1,012) cohorts in an approximately 2:1 ratio. The patients' clinicopathological features were similar between cohorts (**Table S2**). In the development cohort, both univariate and multivariate analysis revealed that HPR was associated with young age (≤45 years), high alpha-fetoprotein (AFP) level (≥400 ng/mL), tumor size >10 cm, >3 tumor nodes, portal vein/hepatic vein tumor thrombosis (PVTT/HVTT), microvascular invasion (MVI), high Ki67 index (≥30%), incomplete tumor capsule, and postoperative complications (all $P < 0.05$) (**Table 1**). Therefore, these 9 variables (age, AFP level, tumor size, tumor nodes, PVTT/HVTT, MVI, Ki67 index, tumor capsule, and postoperative complications) were identified as independent predictors of HPR. The absolute value of the coefficient between each variable did not exceed 0.42 (**Figure 2A**). Multicollinearity analysis revealed that each variable's variance inflation factor did not exceed 2, thus indicating no collinearity among these 9 predictors (**Figure 2B**).



Cohort	Cutoff	Points	Sensitivity	Specificity	PPV	NPV
Development	①	134	95.82%	71.21%	39.39%	98.98%
Development	②	420	13.11%	99.99%	97.50%	85.56%
Validation	①	134	94.65%	70.41%	40.71%	98.13%
Validation	②	420	5.41%	100.0%	100.0%	84.44%

Figure 3 Continued

Preoperative predictive nomogram establishment

Notably, 6 of the 9 predictors above (age, AFP level, tumor size, node numbers, tumor capsule, and PVTT/HVTT status) were available preoperatively. Therefore, to better predict HPR before the operation, we established a preoperative nomogram based on these 6 predictors in the development cohort (**Figure 2C**). Bootstrap validation revealed minimal evidence of model overfitting, given that the C-index of this nomogram was 0.940 (**Figure 2D**). Similar results were obtained for the validation cohort (**Figure S1A**). In addition, ROC curve analysis revealed that the area under the curve values of the preoperative nomogram was 0.940 [95% confidence interval (CI): 92.8%–95.3%] and 0.929 (95% CI: 91.0%–94.8%) in the development and validation cohort, respectively (**Figure 2E**; **Figure S1B**). According to DCA and clinical impact curves, the preoperative nomogram had good predictive efficiency and remarkable predictive power in both cohorts, and a high-risk threshold of 0–0.95 was most beneficial in predicting HPR (**Figure 2F**; **Figure S1C, D**).

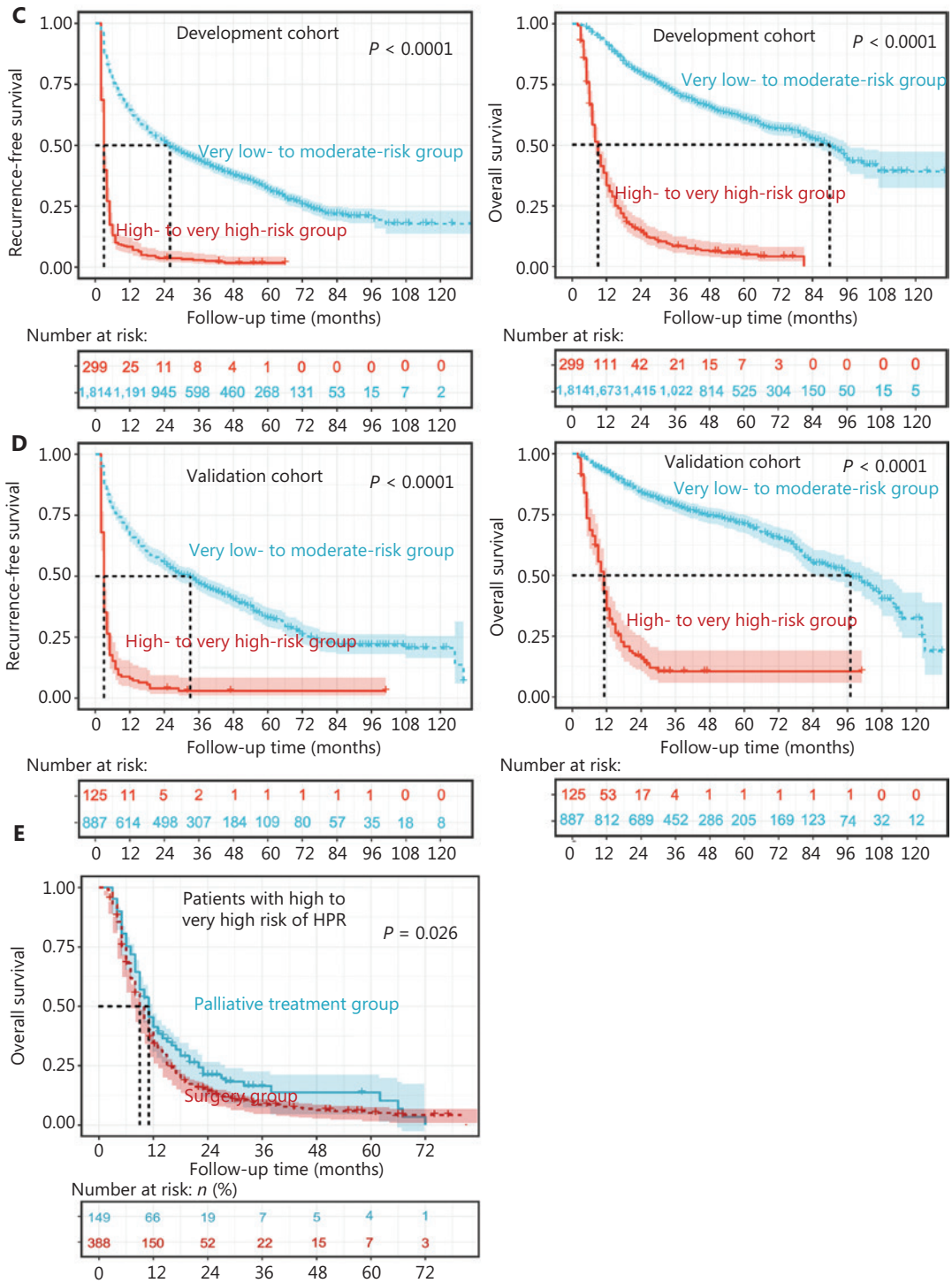


Figure 3 Preoperative HPR risk stratification prediction based on the combination of the preoperative nomogram model with the CTREE model. (A) Identification of the optimal cutoff values for very low and very high HPR risk, predicted with the preoperative nomogram model in both cohorts. (B) Conditional inference tree of HPR risk stratification for patients with scores of 134–420. The 12 terminal nodes show the proportion of HPR. (C, D) Comparison of RFS and OS between patients with high to very high HPR risk *vs.* very low to moderate HPR risk in both cohorts; (E) Comparison of OS in patients with high to very high HPR risk between the palliative treatment group and surgical group..

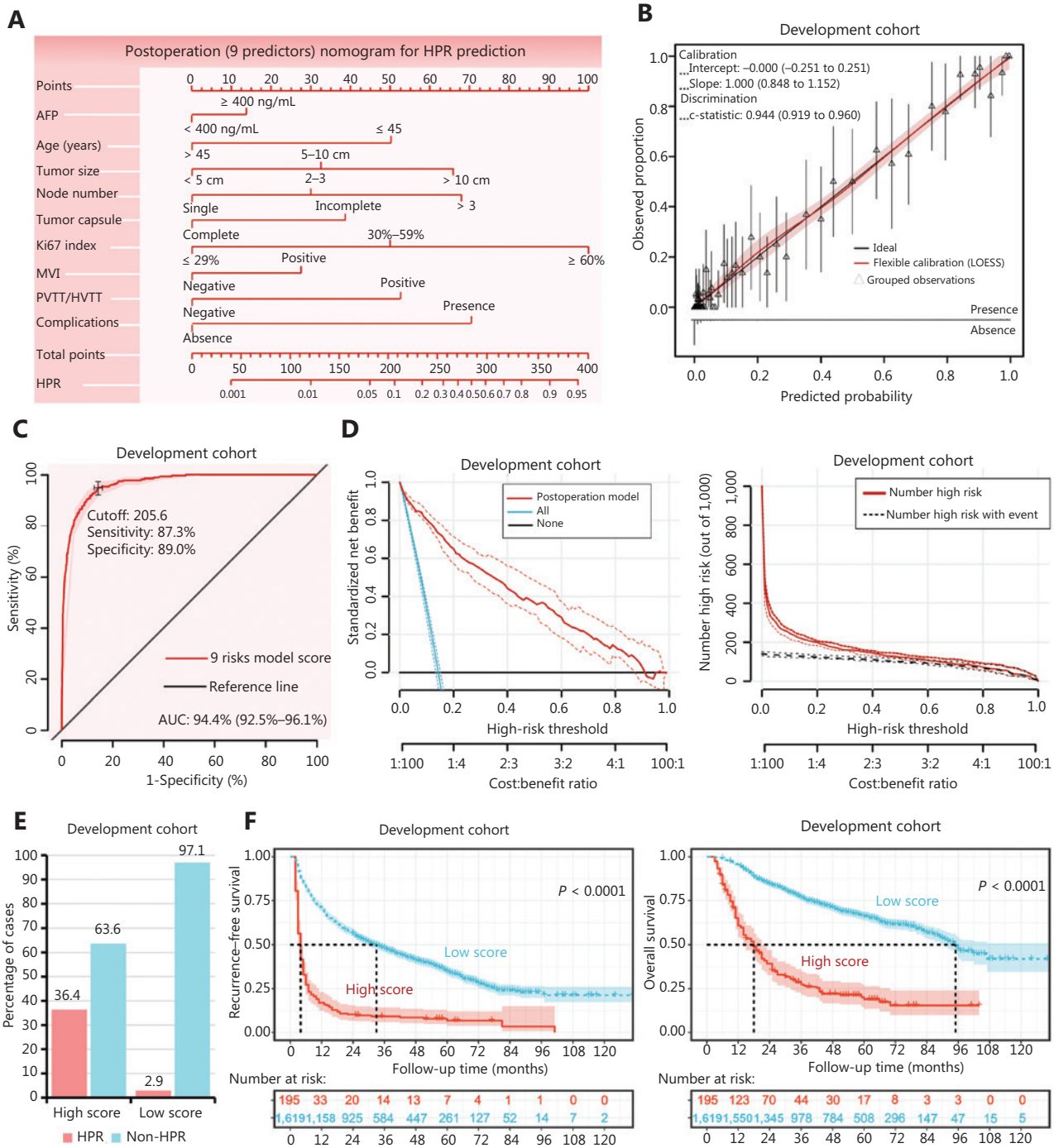


Figure 4 Postoperative nomogram prediction model of HPR establishment and predictive performance evaluation. (A) Postoperative nomogram model for HPR prediction based on the nine total predictors. (B) Calibration plots of the postoperative nomogram model in the development cohort. (C) ROC curve analyses indicating good HPR predictive performance of the postoperative nomogram model in the development cohort. (D) DCA and clinical impact curves of the postoperative nomogram model for predicting HPR in the development cohort. (E) Comparison of HPR rates according to the postoperative nomogram cutoff score (205.6) in the development cohort. (F) Comparison of RFS and OS according to the postoperative nomogram cutoff score (205.6) in the development cohort.

Combination of the preoperative nomogram and CTREE model for preoperative HPR risk assessment

According to the preoperative nomogram, when the cutoff value of predicted HPR incidence was set at 5%, the corresponding total nomogram score was 134, and the negative predictive value (98.98% and 98.13% in the development and validation cohorts, respectively) and sensitivity (95.82% and 94.65% in the development and validation cohorts, respectively) were extremely high at this score (**Figure 3A**). When the cutoff value of predicted HPR incidence was set at 95%, the corresponding total nomogram score was 420, and the positive predictive value (97.50% and 100% in the development and validation cohorts, respectively) and specificity (99.99% and 100% in the development and validation cohorts, respectively) were extremely high at this score (**Figure 3A**). Furthermore, similar very low (or very high) predicted incidence and actual incidence corresponded to these 2 score points in both cohorts. Therefore, the preoperative nomogram indicated that patients with total scores of <134 or >420 had very low risk or very high risk of HPR, respectively.

However, when the patient score was 134–420, prediction errors were observed. **Table S3** shows similar scores between patients 1 and 2; 3 and 4; 5 and 6; 7 and 8; and 9 and 10. However, their actual outcomes differed. Therefore, patients with scores of 134–420 were considered to be at potential risk of HPR, and HPR risk stratification could not be performed on the basis of the nomogram score alone. Consequently, we constructed a CTREE model to further aid in risk stratification and clinical decision-making for the 1,027 patients with scores of 134–420 (**Figure 3B**). Overall, 12 terminal nodes representing different risk hierarchies were identified with the CTREE model. Patients in nodes 1, 2, 3, and 6 were considered to have high HPR risk (> 60%), whereas those in nodes 4, 7, 8, and 9 were considered to have moderate risk (20%–60%), and those in nodes and 5, 10, 11, and 12 were considered to have low risk (< 20%) (**Figure 3B**). As presented in **Table S3**, 4 patients (in nodes 3, 5, 7, and 9) among the 5 patients with HPR were ultimately assigned to the high-risk group, thus reflecting the rationality of the CTREE model.

From the preoperative nomogram combined with the CTREE model, 424 patients (299 and 125 in the development and validation cohorts, respectively) were classified as having high to very high HPR risk. The actual HPR incidence in these patients was 73.6% (220/299) and 76.0% (95/125) in the development and validation cohorts, respectively. Survival analysis indicated that patients with high to very high HPR risk had significantly shorter RFS and OS than those with very low to moderate risk in both cohorts (**Figure 3C, D**). In addition, we retrospectively collected a control cohort of patients (from Guangxi Medical University Cancer Hospital, First Affiliated Hospital of Guangxi Medical University, and Wuming Hospital of Guangxi Medical University) with high to very high HPR risk, who underwent only palliative treatment (e.g., TACE/HIAC, radiotherapy, or systemic treatment). Details of the cohort are shown in **Table S4**. The surgical group displayed a significantly shorter OS than the palliative treatment group (**Figure 3E**). Therefore, for patients with preoperatively predicted high to very high HPR risk, surgery can be considered not to provide benefits.

Postoperative predictive nomogram model establishment and values

Except for the 424 patients with high to very high HPR risk, the remaining 2,701 patients had very low to moderate HPR risk. For such patients, surgical recommendations should be specific to the situation. If all patients with very low to moderate HPR risk were to undergo surgery, HPR would still occur at some rate. Consequently, we constructed a postoperative nomogram for HPR prediction based on all 9 predictors (**Figure 4A**). The C-index of the postoperative nomogram was 0.944 and 0.942 in the development and validation cohorts, respectively (**Figure 4B**; **Figure S2A**). Multi-dimensional verification, including ROC analysis, DCA, and clinical impact curves, also confirmed the predictive accuracy and reliability of the postoperative nomogram in both cohorts (**Figure 4C, D**; **Figure S2B–D**).

Furthermore, according to maximization of the Youden index, the best cutoff score was 205.6, and the sensitivity and specificity were 87.3% and 89.0%, respectively, in the development cohort and 75.1% and 89.8%, respectively, in the validation cohort. Therefore, with a threshold score of 205.6 post-surgery, patients with high scores (>205.6) had significantly higher HPR rates, and lower RFS and OS, than those with low scores (≤205.6) (**Figure 4E, F**). Similar results were obtained in the validation cohort based on the same cutoff score in the development cohort (**Figure S3A–C**).

In addition, postoperative adjuvant (PA)-TACE/HAIC is a common adjuvant therapy for recurrence prevention of

HCC after hepatectomy. Notably, among patients with high scores (>205.6), those who received PA-TACE/HAIC in the early period after surgery displayed lower HPR rates, and significantly longer RFS and OS, than those without PA-TACE/HAIC, in both the development (**Figure S4A–C**) and validation cohorts (**Figure S4D–F**). These findings indicated that early post-operative adjuvant therapies decrease the incidence of HPR and improve prognosis.

Biological function profiles of HCCs with HPR

To better explore the molecular characteristics underlying HPR, we performed whole-transcriptome expression profiling based on RNA sequencing for 119 HCCs (in 31 patients with HPR and 88 patients without HPR, respectively). First, gene set enrichment analysis (GSEA) demonstrated that many cancer-related process clusters were enriched in patients with HPR, including cancer development-related, cellular process-related, metabolism-related, and immune-related clusters (**Figure 5A**; **Table S5**). With the non-HPR group as a reference, we identified 4,986 differentially expressed genes (DEGs) ($\log_2$FC >0, P <0.05) (**Figure 5B**). Weighted gene co-expression network analysis (WGCNA) was used to construct the co-expression network for these 4,986 DEGs, with a soft threshold power (β) value of 5 and a scale-free network (**Figure S5A, B**). The co-expression modules were generated with dynamic tree cutting, and 23 modules were determined (**Figure 5C**). Module cluster analysis revealed that several modules had similar expression profiles. For instance, in modules ME7–13, the DEGs clustered in cellular processes and cancer-related pathways, whereas in modules ME16–19 and ME14–15, most DEGs were enriched in metabolism-related pathways and immune-related pathways, respectively (**Figure 5D**). Module trait relationships revealed that modules ME9 and ME11 were positively correlated with HPR, as well as several malignancy-related clinicopathologic factors (e.g., high AFP level, large tumor size, high Ki67, and PVTT/HVTT), whereas modules ME15 and ME19 were negatively correlated with HPR (**Figure 5D**). GO and KEGG pathway analyses of DEGs in these modules are illustrated in **Figure 5E**. The hub genes of these modules, according to cytoHubba analysis, are illustrated in **Figure 5F**. In addition, with ssGSEA based on immune-related gene sets from the Broad Institute gene-set enrichment database, HCCs with HPR were characterized primarily by immunodeficient or immunosuppressive signatures (**Figure S6A**). Details of each immune infiltrate status "enrichment score" are illustrated in **Figure S6B**. The findings were consistent with the GSEA and WGCNA results described above.

The MYCN/HMGA2 co-expression phenotype enables identification of HCC and its malignant biological characteristics

Two hub genes in modules ME9 and ME11, *MYCN* and *HMGA2*, interacted with many DEGs in these 2 modules (**Figure 6A**). Heatmaps of DEGs revealed that most of these DEGs were up-regulated in patients with rather than without HPR (**Figure 6A**). GO and KEGG pathway analyses of these DEGs revealed that they were enriched primarily in cellular processes and embryonic stem cell development-related processes, and participated in multiple proto-oncogene-related and EMT-related pathways (e.g., *PI3K-AKT*, *P53*, *Hedgehog*, *Wnt*, and *Hippo* signaling pathways) (**Figure 6B**). In addition, high frequency co-expression of *MYCN/HMGA2* was found in patients with HPR, according to RNA-sequencing data of 119 HCCs (**Figure 6C**). Immunofluorescence analysis of MYCN/HMGA2 co-expression was also performed in HCC tissues to provide validation (**Figure 6D**). Log-rank tests among 119 patients indicated that patients with *MYCN/HMGA2*-double high expression (both log FPMK+1 of *MYCN* and *HMGA2* > median) had the lowest RFS and OS among sub-types, particularly with respect to *MYCN/HMGA2*-double negative patients (**Figure 6E**).

To better display the molecular characteristics of *MYCN/HMGA2* co-expression cell subsets in HCC, we performed single-cell RNA sequencing analysis on 27,999 single cells derived from 4 HCCs (*MYCN/HMGA2*-double high expression HCC; only *MYCN* high expression HCC; only *HMGA2* high expression HCC; and *MYCN/HMGA2*-double negative HCC) and 2 adjacent tissues. Nine distinct cell types, including epithelial, endothelial, immune (T cell, B cell, NK cell, etc.), and stromal cells, were assigned known marker genes (**Figure 6F i**), and the proportion of each cell type markedly varied by sample (**Figure 6F ii**). On the basis of copy number variation analysis, 8 main malignant sub-clusters were identified in the epithelial cells (**Figure 6F iii**). *MYCN* expression was concentrated in sub-clusters 1, 3, and 5; whereas *HMGA2* expression was concentrated in sub-clusters 0, 1, 3, and 6. Sub-clusters 1 and 3 were the *MYCN/HMGA2* co-expression sub-clusters (**Figure 6F iv**). Notably,

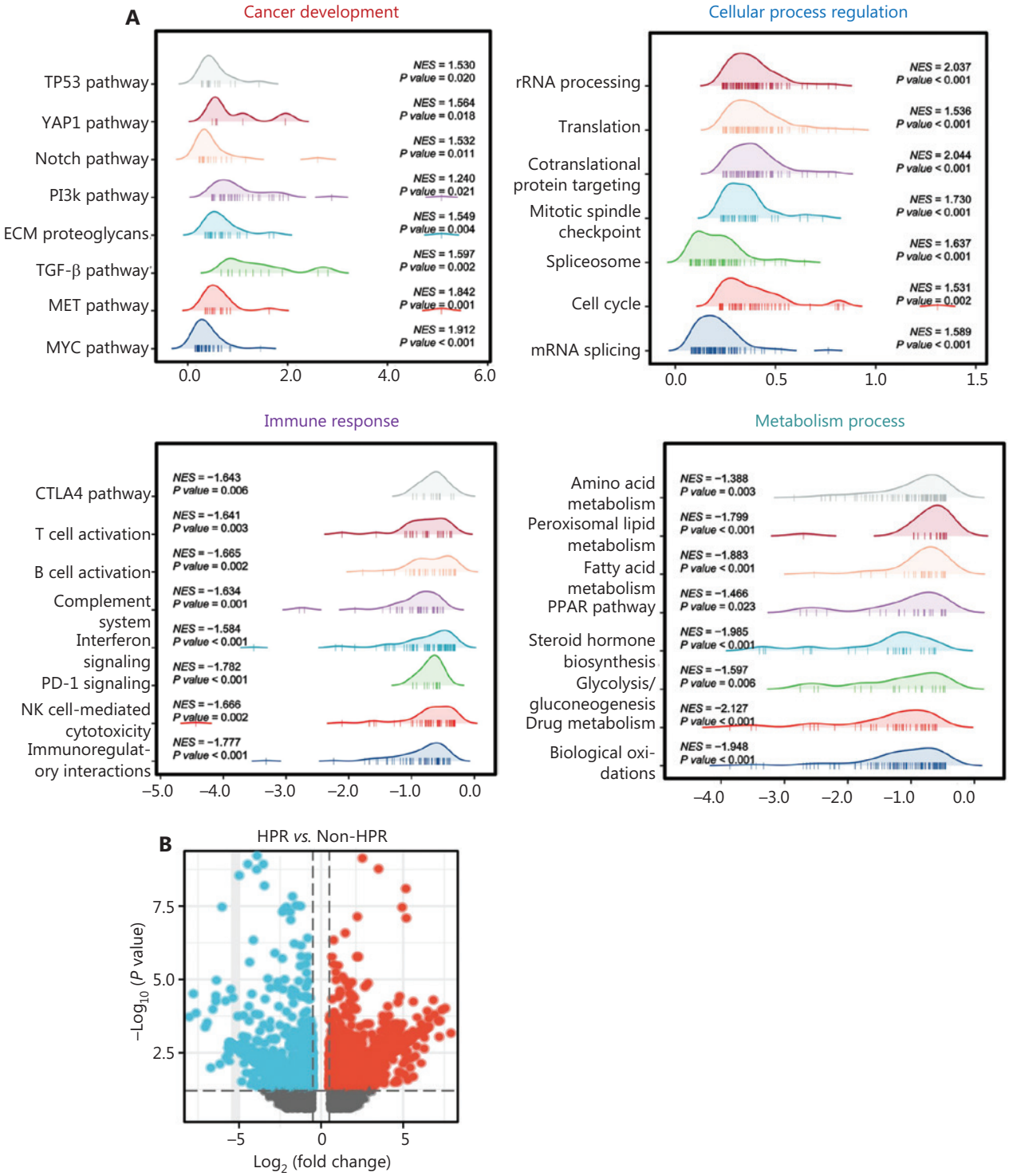
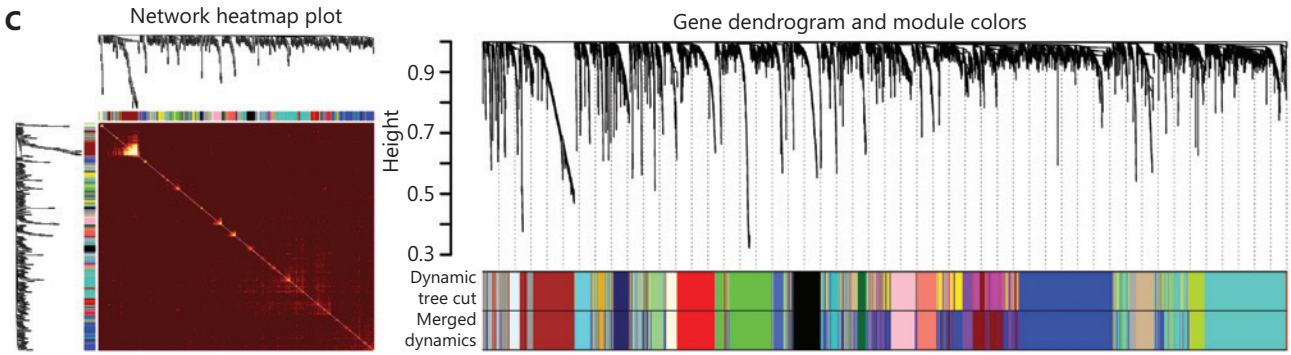
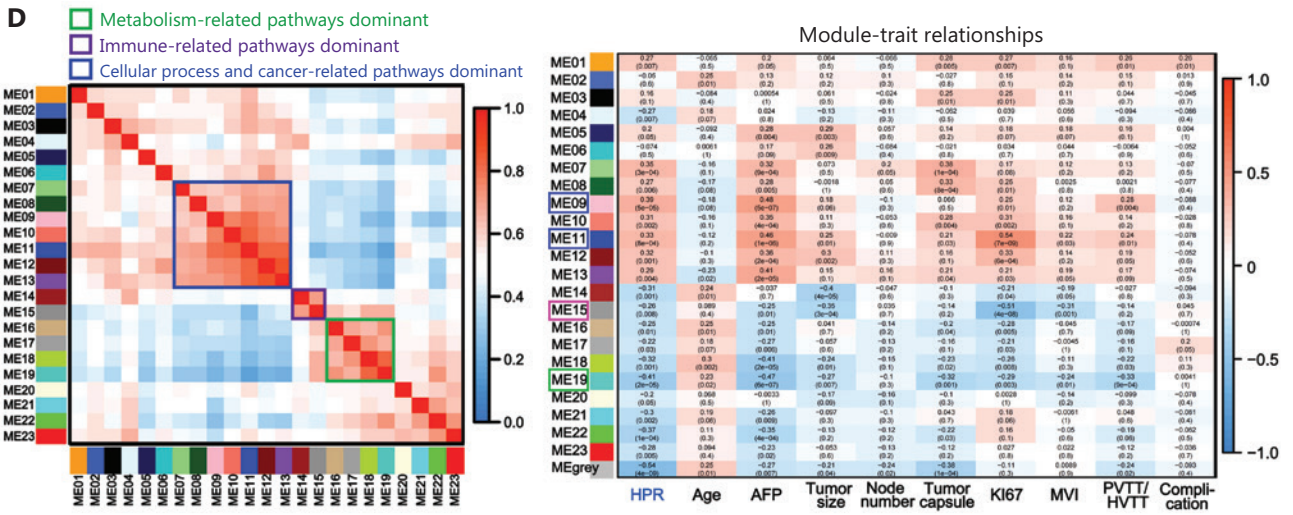
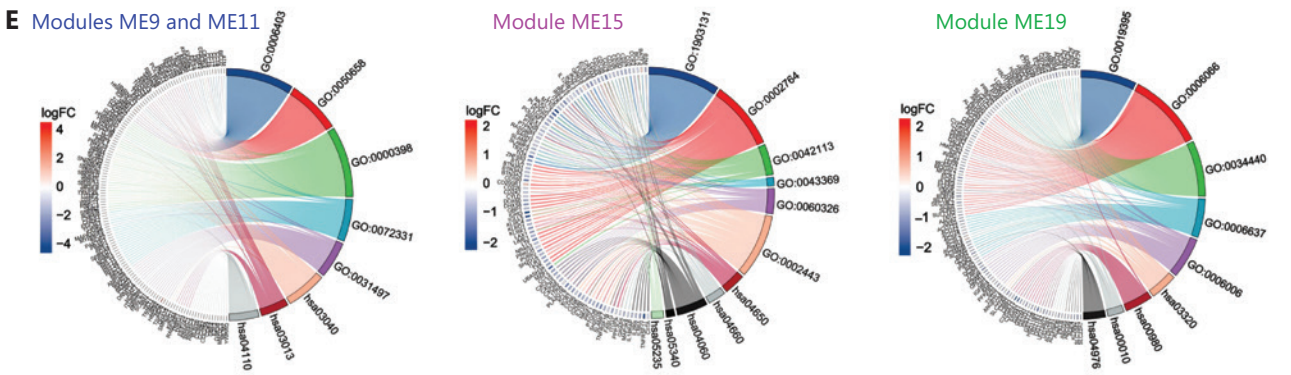


Figure 5 Continued

several mesenchymal markers (*CDH*, *VIM*, and *IGF2BP1*) and stem cell markers (*EpCAM*, *C-MYC*, and *CD44*) had high expression in these 2 sub-clusters (1 and 3), thus indicating the EMT characteristics and CSC phenotype of the *MYCN/HMGA2* co-expression sub-clusters (**Figure S7**). Sub-cluster 3 was also characterized by high expression of







ONTOLOGY	ID	Description
BP	GO:0006403	RNA localization
BP	GO:0050658	RNA transport
BP	GO:0000398	mRNA splicing, *via* spliceosome
BP	GO:0072331	Signal transduction by p53 class mediator
BP	GO:0031497	Chromatin assembly
KEGG	hsa03040	Spliceosome
KEGG	hsa03013	Nucleocytoplasmic transport
KEGG	hsa04110	Cell cycle

ONTOLOGY	ID	Description
BP	GO:1903131	Mononuclear cell differentiation
BP	GO:0002764	Immune response
BP	GO:0042113	B cell activation
BP	GO:0043369	CD4 or CD8 positive
BP	GO:0060326	Cell chemotaxis
BP	GO:0002443	Leukocyte-mediated immunity
KEGG	hsa04650	NK cell-mediated cytotoxicity
KEGG	hsa04660	T cell receptor signaling
KEGG	hsa04060	Cytokine-cytokine receptor interaction
KEGG	hsa05340	Primary immunodeficiency
KEGG	hsa05235	PD-L1/PD-1 checkpoint pathway in cancer

ONTOLOGY	ID	Description
BP	GO:0019395	Fatty acid oxidation
BP	GO:0006066	Alcohol metabolic process
BP	GO:0034440	Lipid oxidation
BP	GO:0006637	Acyl-CoA metabolic process
BP	GO:0006006	Glucose metabolic process
KEGG	hsa03320	PPAR signaling pathway
KEGG	hsa00980	Metabolism of xenobiotics by cytochrome P450
KEGG	hsa00010	Glycolysis/gluconeogenesis
KEGG	hsa04976	Bile secretion

Figure 5 Continued

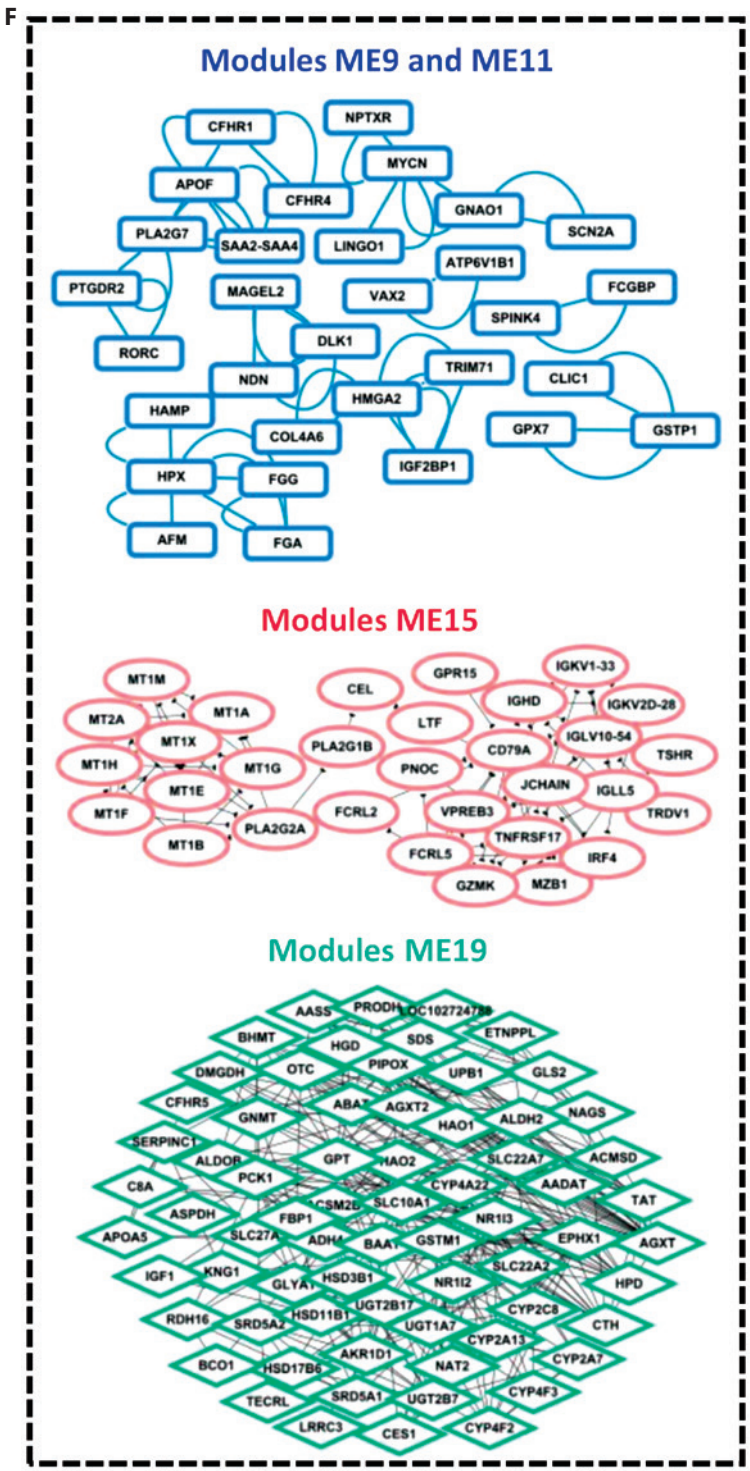


Figure 5 Differential gene expression and biological function profiles of HCCs with HPR. (A) GSEA indicating enrichment of many cancer-related process clusters in patients with HPR. (B) Volcano plot of expression profiles of 4,986 DEGs in HCC between HPR and non-HPR groups. (C) Identification of co-expressed gene modules for 4,986 DEGs in weighted gene co-expression network analysis. (D) Heatmap plot of the adjacencies of modules and association with three cancer-related pathway clusters, and heatmap of the correlations of module eigengenes with HPR and nine clinicopathologic factors. (E) Detailed information on the GO and KEGG pathways enriched in DEGs in modules ME9 and ME11, and ME15 and ME19. (F) PPI networks of hub genes in modules ME9 and ME11, and ME15 and ME19.

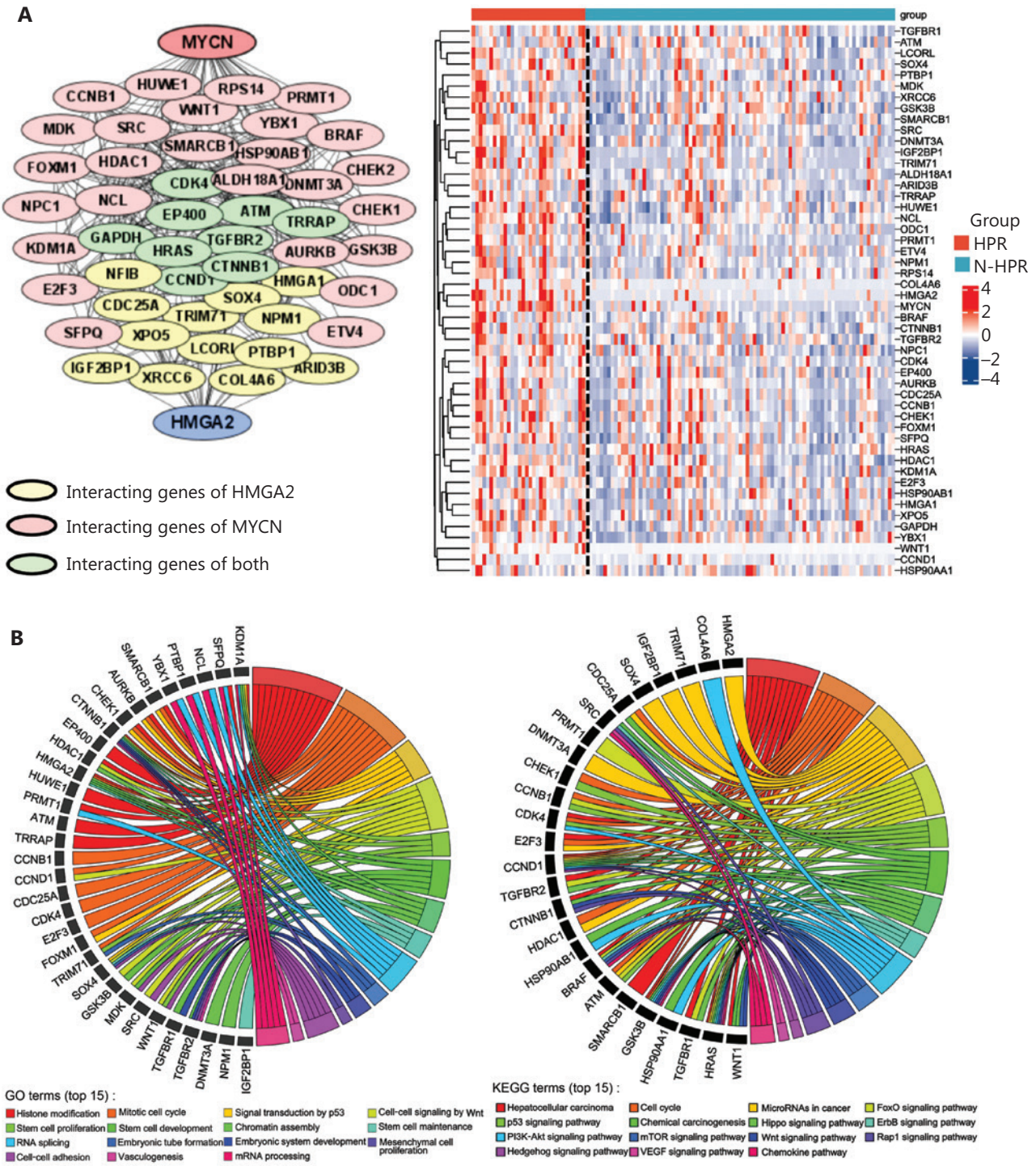


Figure 6 Continued

proliferation-associated genes (*CCNB1*, *CCNB2*, and *MKI67*) (**Figure S7**). In addition, gene set variation analysis revealed the signature heterogeneity among 8 sub-clusters (**Figure 6F v**). The 2 *MYCN/HMGA2* co-expression sub-clusters shared common activated signatures, such as *Wnt* and *TGF-β* signals, alongside unique signatures such as *E2E* target, *MYC* target, and cell cycle (G2M) checkpoint signals in only sub-cluster 3 (**Figure 6F v**).

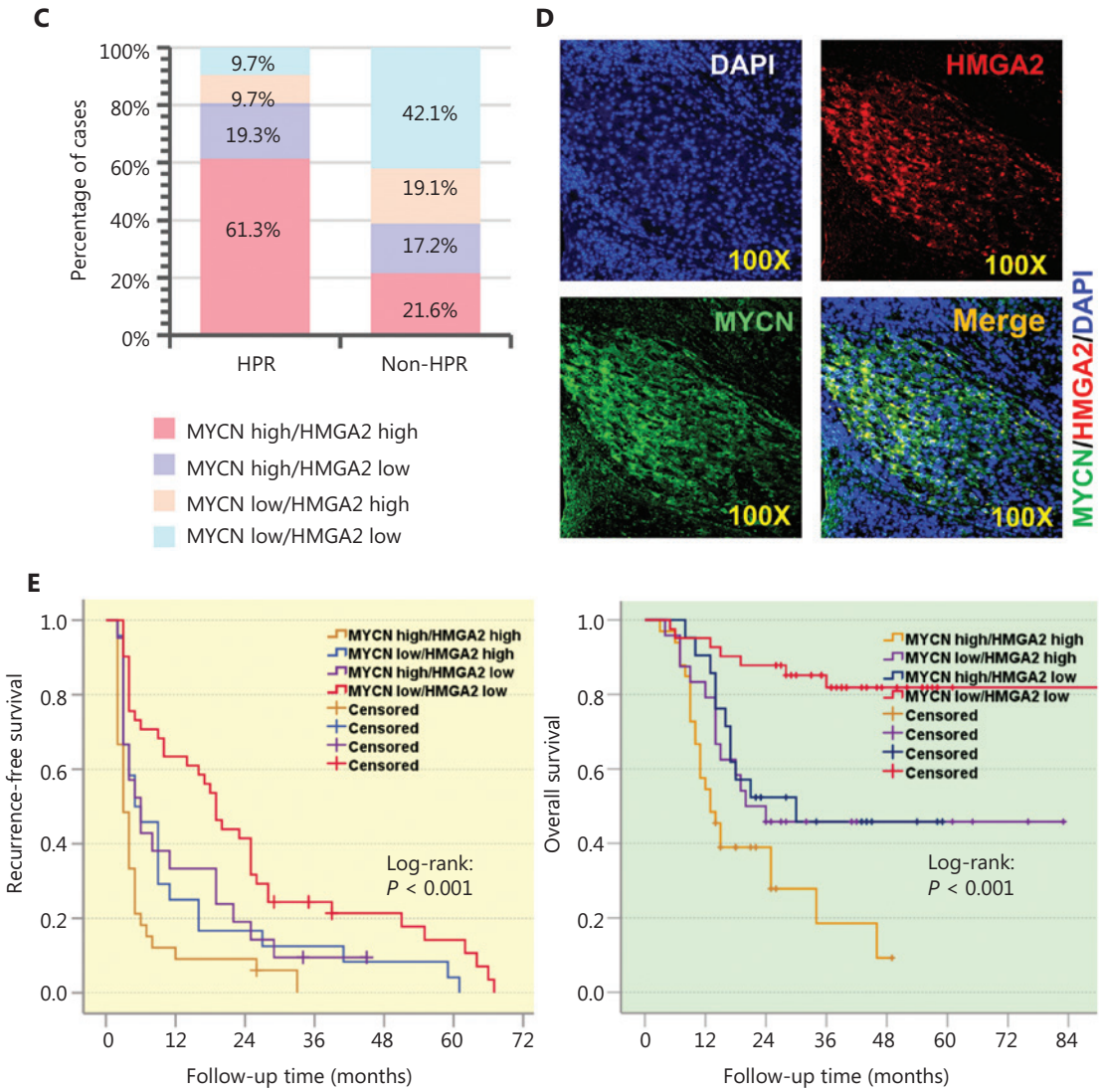


Figure 6 Continued

Treatment patterns and efficacy analysis in patients after HPR

As described previously, among the 506 patients with HPR, 271 (53.6%) received palliative treatment, and 235 (46.4%) received only supportive care. Post-recurrence survival (PFS) analysis was conducted to assess the efficacy of various treatment modalities after HPR. Patients who received palliative treatments had a longer median PFS (6 months) than patients who received only supportive care (3 months) (P <0.001) (**Figure S8A**). Among palliative treatment patterns, the combination therapy modalities achieved the longest PFS in both HPR type A and type B (P <0.001) (**Figure S8B, C**). In addition, for HPR type A, locoregional therapies achieved better PFS than systemic therapies; for HPR type B, systemic therapies performed slightly better than locoregional therapies (**Figure S8B, C**).

In addition, *MYCN* and *HMGA2* mRNA levels were analyzed with qRT-PCR in 159 patients with HPR. According to the expression level (−ΔΔCT) in tumor tissues, 159 patients were further subdivided into a *MYCN/HMGA2*-double high expression group (both mRNA level ≥ mean level, n = 54), a *MYCN* or *HMGA2* high expression group (n = 52), and a *MYCN/HMGA2*-double low expression group (both mRNA level < mean level, n = 53). PFS was significantly longer in patients with *MYCN/HMGA2*-double low expression who

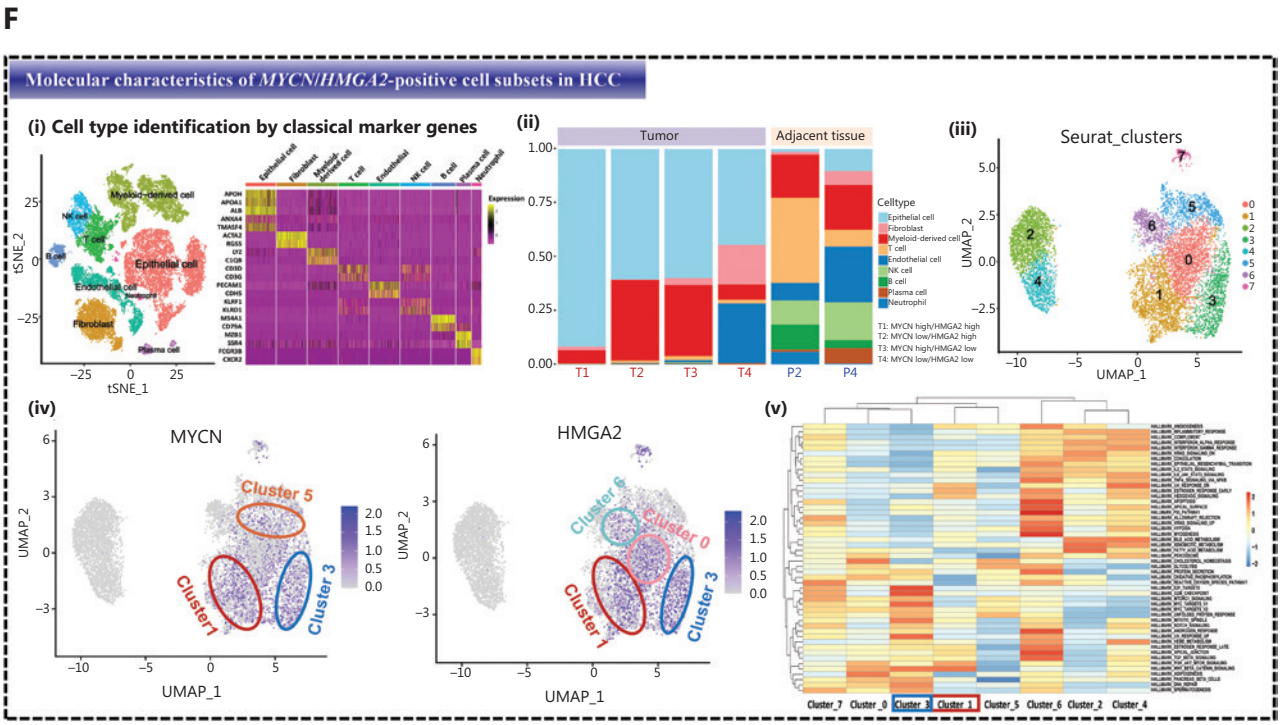


Figure 6 The MYCN/HMGA2 co-expression phenotype for HCC identification and analysis of its malignant biological characteristics. (A) Interaction network of DEGs interacting with MYCN and HMGA2 in modules ME9 and ME11, and heatmap of DEGs interacting with MYCN and HMGA2 in patients with *vs.* without HPR. (B) GO and KEGG pathway analyses of these DEGs, indicating enrichment primarily in cellular processes and embryonic stem cell development-related processes, and participation in multiple proto-oncogene-related and EMT-related pathways. (C) Comparison of the percentages of each subtype according to *MYCN/HMGA2* expression (log FPMK+1) between HPR and non-HPR groups in 119 patients. (D) Representative immunofluorescence MYCN/HMGA2 co-expression patterns in HCC tissue. (E) Comparison of RFS and OS among the four subtypes, according to *MYCN/HMGA2* expression in 119 patients. (F) Molecular characteristics of MYCN/HMGA2-positive cell subsets in HCC: (i) tSNE plots for the eight cell types identified from four HCCs and two adjacent tissues, and heatmap showing 21 marker genes for eight distinct cell types. (ii) Bar plots showing the proportions of cell types in each sample. (iii) tSNE plots for eight main malignant sub-clusters from the re-clustering of the epithelial cells. (iv) UMAP plots showing the major sub-clusters of *MYCN* and *HMGA2* in eight distinct malignant sub-clusters. (v) Differences in pathway activity (scored per cell by GSVA) in eight distinct malignant sub-clusters.

received palliative treatments than in patients receiving only supportive care ($P = 0.028$), although this finding was not statistically significant in the *MYCN/HMGA2* double-high-expression group ($P = 0.250$) and the *MYCN* or *HMGA2* high expression group ($P = 0.077$) (**Figure S8D–F**). Therefore, high expression of *MYCN/HMGA2* might compromise therapeutic efficacy in patients with HPR.

Summary of clinical strategies for HPR prevention and management

On the basis of our results, we tentatively proposed a comprehensive clinical strategy to guide HPR management from pre-operative decision-making to treatment after HPR (**Figure 7**). Specifically, the pre-operative nomogram model may be used to identify patients not suitable for surgery (patients with very high HPR risk) and those suitable for surgery (patients with very low HPR risk). Patients with a preoperative nomogram score of 134–420 were considered to have potential HPR risk and were further assessed with the CTREE model, which classified them into high-, moderate-, or low-HPR risk categories to optimize surgical decision-making. The postoperative nomogram model could then be used to further assess HPR risk for postoperative patients, to guide early postoperative adjuvant therapies for recurrence prevention. Furthermore, the biological insights into HPR advance knowledge of the molecular factors associated with HPR and may guide treatment choice after HPR.

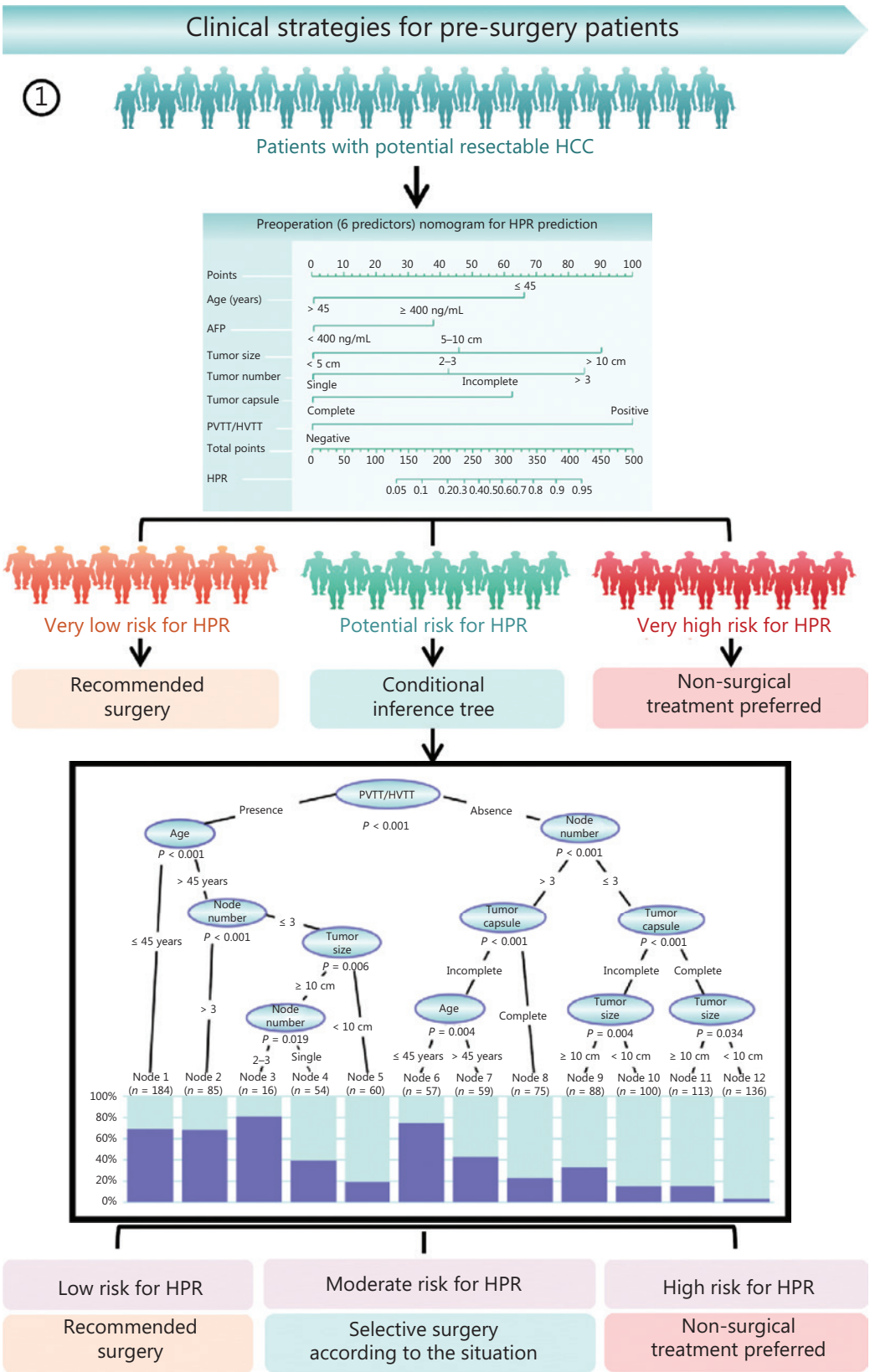


Figure 7 Continued

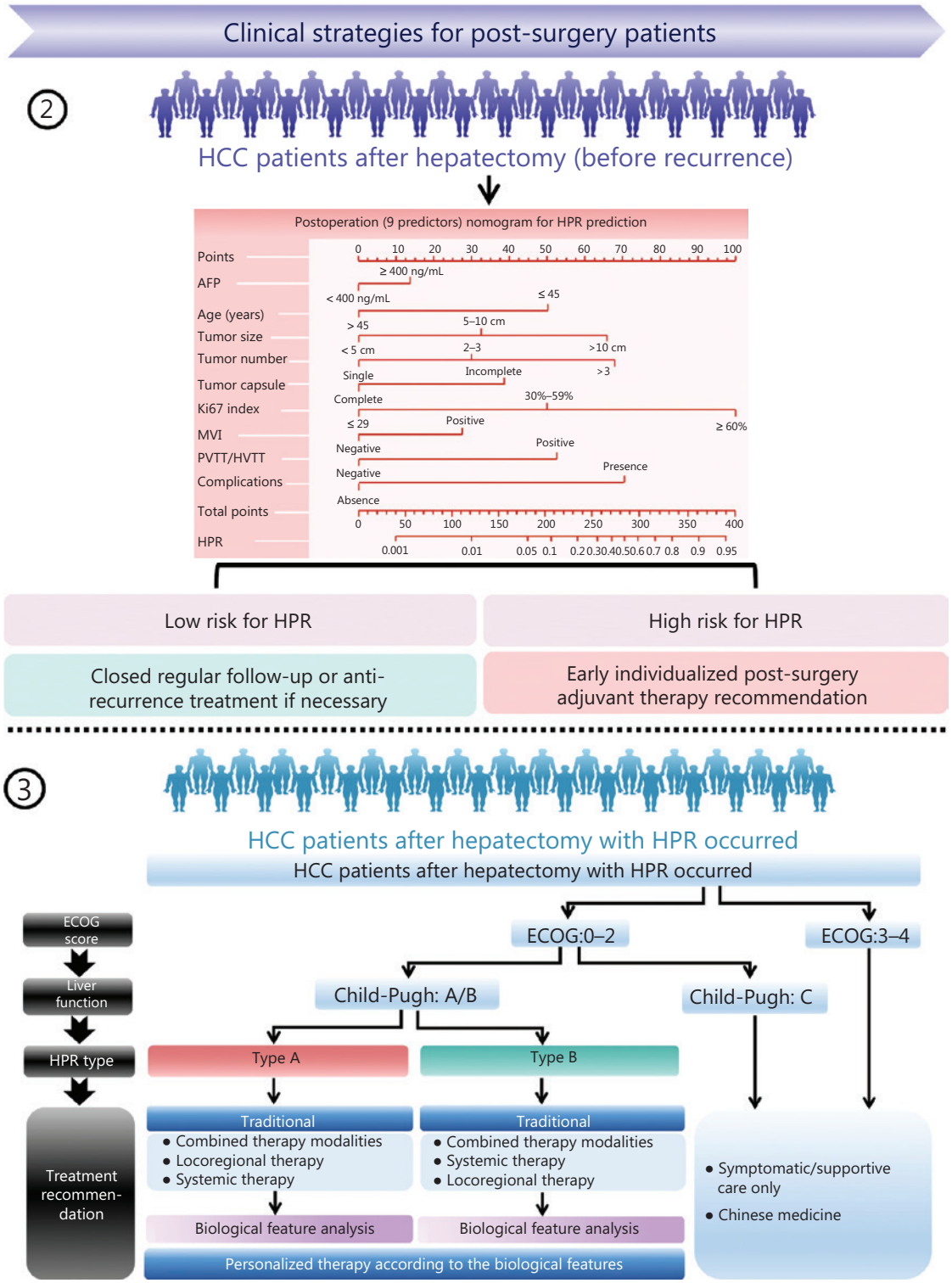


Figure 7 Summary of clinical strategies based on preoperative and postoperative HPR risk assessment. ① Combination of a preoperative nomogram with a CTREE model for the preoperative risk assessment of HPR. ② Postoperative predictive nomogram model establishment and values. ③ Schematic diagram of potential treatment options for patients with HCC after hepatectomy with HPR occurrence.

Discussion

We previously identified a highly specific pattern of early recurrence called HPR[13]. This study further evaluated the characteristics of HPR and its effects on survival in a sufficiently large sample of multicenter data, to capture a consistent and clinically significant fraction of patients. Although the incidence of HPR in the present study was only 16.19%, its influence on patients' poor prognosis was highly significant. Notably, under standardized periodic follow-up after surgery, all HPR cases occur in very early postoperative stages, which is one of the major reasons for extremely poor prognosis. However, unlike most common pattern of early recurrences, HPR exhibits a key feature of sudden simultaneous occurrence of a high recurrence-nodule burden. We observed relatively high ECOG scores (>2) and poor liver function in patients with HPR during recurrence, thus suggesting that the high recurrence-nodule burden adversely influences patients' systemic and liver function, thereby leading to poor OS. Additionally, the limited treatment options for HPR might also contribute to the extremely poor prognosis of HPR.

In this study, we identified 9 clinicopathological factors associated with HPR, which provide an enhanced explanation of HPR occurrence in 3 dimensions. Five factors (large tumor, multi-tumor nodes, incomplete tumor capsule, MVI, and PVTT/HVTT) have been recognized as tumor-related factors reflecting primary tumor invasion features[15-18]. These factors constitute the first-dimensional element of HPR and indicate that wide intrahepatic/extra-hepatic dissemination has occurred preoperatively. Second, high AFP level and Ki67 index may reflect strong primary tumor embryonic-like plasticity and strong proliferation potential[19-21]. These factors may confer a rapidly adaptive and robust proliferative function on metastatic cells, thereby forming a second dimension potentially explaining the "latency-free" nature of HPR. Third, we noted that post-operative complications were the only surgery-related factors for HPR. Postoperative complications can alter the immune microenvironment, thus enabling immune escape and rapid growth of metastatic tumors. Importantly, post-operative complications were the only controllable factor among the 9 identified risk factors. Therefore, greater attention should be paid to improving perioperative management to decrease HPR risk by controlling the incidence of postoperative complications.

Younger patients with HCC tend to have poorer prognosis than older patients[22,23], in agreement with our findings indicating younger age (≤45 years) as a risk factor. The exact reasons for this phenomenon remain unclear but might be partly attributable to younger patients presenting with more advanced stages of HCC at diagnosis, because of limited early screening and follow-up[24,25]. Therefore, regular screening for liver tumors in young adults at high risk of developing HCC, such as those with hepatitis B or C virus (HBV/HCV) infection, is imperative. However, younger patients might also have better liver functional reserves and stronger tolerance than older individuals. Therefore, whenever feasible, resection surgery remains recommended for young patients, particularly those with early-stage HCC with favorable systemic conditions.

A nomogram integrating diverse clinicopathologic factors and gene expression data can generate the individual probability of tumor recurrence or survival in patients with HCC[26-29]. In contrast to previous studies, this study focused on HPR and used an innovative design in which HPR risk factors were identified, and a "model layer pass" method was used to predict and stratify for HPR risk. Specifically, we first established a pre-operative nomogram for HPR prediction based on the 6 variables available pre-operatively. Because of the large sample size of this study, the pre-operative nomogram demonstrated satisfactory predictive power. However, we also considered the limitations of the nomogram, in that it could only weigh the score of each risk factor for each patient but did not account for the effects of different combinations of risk factor stratification on outcome events. Therefore, we further established CTREE model, which offers straightforward visualization of the HPR risk stratification of patients with different combinations of risk factors and provides a decision-making procedure to assign patients. PVTT/HVTT status was identified as the first discriminator among all examined variables, thus suggesting PVTT/HVTT had more pronounced effects than other variables on HPR risk. Notably, with the CTREE model, PVTT/HVTT positive patients were successfully assigned to sub-groups according to high (nodes 1, 2, and 3), moderate (node 4), or low (node 5) HPR risk, thereby providing a basis for deciding on the appropriateness of surgery in patients with advanced stage HCC. Furthermore, the actual HPR incidence in patients with high HPR risk predicted according to the combination of the preoperative nomogram and CTREE model was >70% in both cohorts, thereby reflecting the high efficiency of this preoperative model combination. Survival analysis also confirmed the reliability of the preoperative model combinations in clinical applications.

For patients with high to very high HPR risk, surgery did not result in better OS than other palliative treatments yet exposed patients to surgical trauma. Therefore, concluding that surgery does not benefit patients with high to very high risk of HPR is reasonable, and less invasive and traumatic palliative therapies might be preferred. Recently, encouraging progress has been made in conversion surgery following the combination of multiple preoperative locoregional and systemic therapies for advanced HCC[30-32]. Consequently, the conversion therapy strategy might be a potential option for patients with high risk of HPR; however, further validation is necessary in future prospective research. Very low to low-risk patients may achieve the most surgical benefits. However, surgery should be cautiously recommended for moderate-risk patients after multiple considerations (e.g., surgical risk and patient tolerance). Despite hierarchical decision-making through preoperative model combinations, some patients will still experience postoperative HPR, possibly because of pathological risk factors (e.g., MVI and Ki67) that cannot be included in the preoperative model combinations. Consequently, we established a postoperative nomogram for postoperative HPR prediction, which also showed excellent performance. This nomogram enabled further stratification of postoperative patients and may facilitate decision-making regarding early postoperative adjuvant therapy.

Overall, our "model layer pass" method has potential value in clinical decision-making before and after surgery. The preoperative model combinations may enable accurate identification of patients truly suitable for hepatectomy, thereby increasing surgical effectiveness; whereas the post-operative prediction model may guide the design of postoperative protocols (e.g., postoperative monitoring and early adjuvant therapy). Notably, the 9 variables incorporated into our models are frequently available clinical indicators, thus supporting the feasibility of easy and broad application of our "model layer pass" in clinical practice.

Genomic analysis of primary tumors in patients with HPR may enhance knowledge of the molecular events relevant to HPR. For instance, in this study, HCCs with HPR were characterized by frequent activation of cellular processes and numerous enriched DEGs involved in many cancer invasion/proliferation signaling pathways, including the *Wnt*, *PI3K-AKT*, *TGF-β*, *MYC*, and *Hedgehog* signaling pathways. The hyperactivity of biological processes and the wide activation of multiple cancer proliferation/metastasis-related pathways may partly explain the "latency-free" and "hyper-progression" nature of HPR. Additionally, module trait relationships revealed that modules (ME9 and ME11) containing many cancer invasion/proliferation DEGs were significantly positively correlated with HPR as well as several malignant-related clinicopathologic factors (e.g., high AFP level, large tumor size, high Ki67, and PVTT/HVTT). These findings are consistent with our multivariate analysis results, which indicated that patients with HPR presented 9 related clinicopathologic factors, thus reflecting the rationality of using the 9 factors in our model combinations above.

The *MYCN/HMGA2* co-expression pattern was highly frequent in patients with HPR. *MYCN* encodes an important transcription factor that mediates epigenetic reprogramming and drives lineage plasticity in many cancers[33,34]. *HMGA2* encodes a non-histone architectural transcription factor that modulates the transcription of genes by binding AT-rich sequences, thereby altering chromatin structure (chromatin remodeling) and influencing biological processes[35]. Herein, we observed that *MYCN* and *HMGA2* interacted with numerous cellular process and embryonic stem cell development-related DEGs. Moreover, scRNA-seq analysis revealed the high malignancy potential, including the EMT characteristics, high proliferation, and CSC phenotype, of *MYCN/HMGA2* co-expression cell sub-clusters in HCC. These findings suggested the importance of the *MYCN/HMGA2* co-expression pattern in the development of HPR, and suggested its close association with hyperactive biological processes and widely activated cancer-related pathways in HPR, although the specific mechanism remains unclear.

Compared with supportive care alone, palliative treatment prolonged PFS in patients with HPR. Notably, combination therapy modalities achieved the longest PFS in both HPR type A and type B. Therefore, combination therapy modalities might be preferred for patients with HPR, regardless of type. Nevertheless, the efficacy of traditional treatments for HPR is limited, possibly because of the high frequency co-expression pattern of *MYCN/HMGA2*. However, preclinical studies have shown that HMGA2 inhibitors inhibit the growth of cancer cells and prevent tumor transformation[36]. Additionally, *MYCN* positive HCC is highly sensitive to trans-retinoic acid, because of the high expression of stem markers such as EPCAM[37]. We suggest that the detection of *MYCN/HMGA2* might become a routine procedure in HCC profiling, and targeting of *MYCN/HMGA2* might provide a promising approach for HPR treatment.

This study has several limitations that should be acknowledged. The primary limitation was the difference in sample

sizes between center 1 and other centers, which might have introduced potential bias in the analysis. Furthermore, the study population was recruited exclusively from China and had predominant representation of HBV-related HCC cases, thus limiting the generalizability of our findings to other HCC etiologies. To address these limitations, future research should incorporate 1) prospective collection of balanced sample sizes across multiple centers to enhance statistical power and representation and 2) inclusion of an external validation cohort comprising non-HBV-related HCC (e.g., HCV-related HCC), to verify the robustness of our findings across diverse etiological backgrounds. Additionally, further dimensional molecular research (e.g., proteomics and metabolomics, scATAC-seq, and spatial multi-omics analysis) of HPR should be conducted to provide more precise information regarding the personalized treatment for HPR.

Conclusions

In conclusion, HPR after hepatectomy has extremely poor prognosis, mainly because of its short TTR, large tumor burden, adverse effects on systemic and liver function, and limited therapeutic options. Multivariate analyses revealed 9 clinicopathological factors associated with HPR. Subsequently, comprehensive models for HPR prediction and risk stratification were established, which displayed excellent predictive performance and applicability to formulating pre- and postoperative strategies. Multi-dimensional verification also confirmed the predictive accuracy of the model combinations and their reliability in clinical applications. Biological analyses revealed that HCCs with HPR exhibited hyperactive biological processes, inactive metabolism, and immune exhaustion features, together with high frequency of *MYCN/HMGA2* co-expression, thus enhancing understanding of the molecular events leading to HPR and providing valuable knowledge for guiding HPR therapy. Overall, in this study, we explored the clinicopathological factors and biological features associated with HPR, and propose a comprehensive clinical strategy for guiding HPR prevention and management.

Acknowledgments

We thank Novogene (Beijing, China) for assistance in RNA sequencing and RNA-seq analysis, and Singleron (Nanjing, China) for assistance in single cell RNA sequencing analysis.

Grant support

This work was supported by the National Natural Science Foundation of China (Grant Nos. NSFC 82273405, and 81972306). This work was also supported partly by the Guangxi Nature Sciences grants (Grant No. 2018GXNSFAA138028) and the Guangxi Medical University Training Program for Distinguished Young Scholars.

Conflict of interest statement

No potential conflicts of interest are disclosed.

Author contributions

Conceived and designed the analysis: Lunan Qi, Liang Ma.
Collected the data: Lunan Qi, Zhan Lu, Min Zhou, Yingwu Huang, Yongchi Ling, Hai Huang, Yuchong Peng, Tao Peng, Liang Ma.
Contributed data or analysis tools: Lunan Qi, Jingxuan Xu, Yuanyuan Chen.
Performed the analysis: Jingxuan Xu, Yuanyuan Chen.
Wrote the paper: Lunan Qi, Jingxuan Xu.

Data availability statement

All data included in this study are available upon request by contact with the corresponding author.

References

1. Bray F, Laversanne M, Sung H, Ferlay J, Siegel RL, Soerjomataram I, et al. Global cancer statistics 2022: GLOBOCAN estimates of incidence and mortality worldwide for 36 cancers in 185 countries. CA Cancer J Clin. 2024; 74: 229-63.
2. Tabrizian P, Jibara G, Shrager B, Schwartz M, Roayaie S. Recurrence of hepatocellular cancer after resection: patterns, treatments, and prognosis. Ann Surg. 2015; 261: 947-55.
3. Llovet JM, Kelley RK, Villanueva A, Singal AG, Pikarsky E, Roayaie S, et al. Hepatocellular carcinoma. Nat Rev Dis Primers. 2021; 7: 6.
4. Li SH, Mei J, Cheng Y, Li Q, Wang QX, Fang CK, et al. Postoperative adjuvant hepatic arterial infusion chemotherapy with FOLFOX in hepatocellular carcinoma with microvascular invasion: a multicenter, phase III, randomized study. J Clin Oncol. 2023; 41: 1898-908.
5. Wang Z, Ren Z, Chen Y, Hu J, Yang G, Yu L, et al. Adjuvant transarterial chemoembolization for HBV-related hepatocellular

carcinoma after resection: a randomized controlled study. Clin Cancer Res. 2018; 24: 2074-81.
6. Wang WH, Wang Z, Wu JX, Zhang T, Rong WQ, Wang LM, et al. Survival benefit with IMRT following narrow-margin hepatectomy in patients with hepatocellular carcinoma close to major vessels. Liver Int. 2015; 35: 2603-10.
7. Lee JH, Lee JH, Lim YS, Yeon JE, Song TJ, Yu SJ, et al. Adjuvant immunotherapy with autologous cytokine-induced killer cells for hepatocellular carcinoma. Gastroenterology. 2015; 148: 1383-91.
8. Xia Y, Li J, Liu G, Wang K, Qian G, Lu Z, et al. Long-term effects of repeat hepatectomy vs percutaneous radiofrequency ablation among patients with recurrent hepatocellular carcinoma: a randomized clinical trial. JAMA Oncol. 2020; 6: 255-63.
9. Peng Z, Chen S, Wei M, Lin M, Jiang C, Mei J, et al. Advanced recurrent hepatocellular carcinoma: treatment with sorafenib alone or in combination with transarterial chemoembolization and radiofrequency ablation. Radiology. 2018; 287: 705-14.
10. Ali R, Riaz A, Gabr A, Abouchaleh N, Mora R, Al Asadi A, et al. Clinical outcomes of Y90 radioembolization for recurrent hepatocellular carcinoma following curative resection. Eur J Nucl Med Mol Imaging. 2017; 44: 2195-202.
11. Lou J, Li Y, Liang K, Guo Y, Song C, Chen L, et al. Hypofractionated radiotherapy as a salvage treatment for recurrent hepatocellular carcinoma with inferior vena cava/right atrium tumor thrombus: a multi-center analysis. BMC Cancer. 2019; 19: 668.
12. Zhuang L, Mou HB, Yu LF, Zhu HK, Yang Z, Liao Q, et al. Immune checkpoint inhibitor for hepatocellular carcinoma recurrence after liver transplantation. Hepatobiliary Pancreat Dis Int. 2020; 19: 91-3.
13. Qi L-N, Ma L, Wu F-X, Chen Y-Y, Xu J-X, Peng Y-C, et al. Clinical implications and biological features of a novel postoperative recurrent HCC classification: a multi-centre study. Liver Int. 2022; 42: 2283-98.
14. Zhou J, Sun H-C, Wang Z, Cong W-M, Zeng M-S, Zhou W-P, et al. Guidelines for the diagnosis and treatment of primary liver cancer (2022 edition). Liver Cancer. 2023; 12: 405-44.
15. Lu XY, Xi T, Lau WY, Dong H, Xian ZH, Yu H, et al. Pathobiological features of small hepatocellular carcinoma: correlation between tumor size and biological behavior. J Cancer Res Clin Oncol. 2011; 137: 567-75.
16. Liang BY, Gu J, Xiong M, Zhang EL, Zhang ZY, Chen XP, et al. Tumor size may influence the prognosis of solitary hepatocellular carcinoma patients with cirrhosis and without macrovascular invasion after hepatectomy. Sci Rep. 2021; 11: 16343.
17. Calderaro J, Petitprez F, Becht E, Laurent A, Hirsch TZ, Rousseau B, et al. Intra-tumoral tertiary lymphoid structures are associated with a low risk of early recurrence of hepatocellular carcinoma. J Hepatol. 2019; 70: 58-65.
18. Erstad DJ, Tanabe KK. Prognostic and therapeutic implications of microvascular invasion in hepatocellular carcinoma. Ann Surg Oncol. 2019; 26: 1474-93.
19. Ma WJ, Wang HY, Teng LS. Correlation analysis of preoperative serum alpha-fetoprotein (AFP) level and prognosis of hepatocellular carcinoma (HCC) after hepatectomy. World J Surg Oncol. 2013; 11: 212.
20. Scholzen T, Gerdes J. The Ki-67 protein: from the known and the unknown. J Cell Physiol. 2000; 182: 311-22.
21. Mrouj K, Andrés-Sánchez N, Dubra G, Singh P, Sobecki M, Chahar D, et al. Ki-67 regulates global gene expression and promotes sequential stages of carcinogenesis. Proc Natl Acad Sci USA. 2021; 118: e2026507118.
22. Diao YK, Liu JW, Wu H, Wang MD, Fan XP, Chen TH, et al. Long-term oncologic outcomes of liver resection for hepatocellular carcinoma in adolescents and young adults: a multicenter study from a hepatitis B virus-endemic area. Am J Surg. 2021; 222: 751-8.
23. Xu XS, Chen W, Miao RC, Zhou YY, Wang ZX, Zhang LQ, et al. Survival analysis of hepatocellular carcinoma: a comparison between young patients and aged patients. Chin Med J (Engl). 2015; 128: 1793-800.
24. Kim JH, Choi MS, Lee H, Kim DY, Lee JH, Koh KC, et al. Clinical features and prognosis of hepatocellular carcinoma in young patients from a hepatitis B-endemic area. J Gastroenterol Hepatol. 2006; 21: 588-94.
25. Aramaki M, Kawano K, Sasaki A, Ohno T, Tahara K, Kai S, et al. Hepatocellular carcinoma in young adults. Hepatogastroenterology. 2005; 52: 1795-7.
26. Zhang ZJ, Wei BJ, Liu ZK, Xuan ZF, Zhou L, Zheng SS. Nomogram for prediction of hepatocellular carcinoma recurrence after liver resection. Hepatobiliary Pancreat Dis Int. 2025; 24: 269-76.
27. Fang Q, Yang R, Chen D, Fei R, Chen P, Deng K, et al. A novel nomogram to predict prolonged survival after hepatectomy in repeat recurrent hepatocellular carcinoma. Front Oncol. 2021; 11: 646638.
28. Liu WR, Tian MX, Tang Z, Fang Y, Zhou YF, Song SS, et al. Nine-factor-based immunohistochemistry classifier predicts recurrence for early-stage hepatocellular carcinoma after curative resection. Br J Cancer. 2020; 123: 92-100.
29. Xu W, Li R, Liu F. Novel prognostic nomograms for predicting early and late recurrence of hepatocellular carcinoma after curative hepatectomy. Cancer Manag Res. 2020; 12: 1693-712.
30. Kaseb AO, Hasanov E, Cao HST, Xiao L, Vauthey JN, Lee SS, et al. Perioperative nivolumab monotherapy versus nivolumab plus ipilimumab in resectable hepatocellular carcinoma: a randomised, open-label, phase 2 trial. Lancet Gastroenterol Hepatol. 2022; 7: 208-18.
31. Chiang CL, Chiu KWH, Chan KSK, Lee FAS, Li JCB, Wan CWS, et al. Sequential transarterial chemoembolisation and stereotactic body radiotherapy followed by immunotherapy as conversion therapy for patients with locally advanced, unresectable hepatocellular carcinoma (START-FIT): a single-arm, phase 2 trial. Lancet Gastroenterol Hepatol. 2023; 8: 169-78.
32. Arita J, Ichida A, Nagata R, Mihara Y, Kawaguchi Y, Ishizawa T, et al. Conversion surgery after preoperative therapy for advanced hepatocellular carcinoma in the era of molecular targeted therapy and immune checkpoint inhibitors. J Hepatobiliary Pancreat Sci. 2022; 29: 732-40.

33. Dardenne E, Beltran H, Benelli M, Gayvert K, Berger A, Puca L, et al. N-Myc induces an EZH2-mediated transcriptional program driving neuroendocrine prostate cancer. Cancer Cell. 2016; 30: 563-77.
34. Berger A, Brady NJ, Bareja R, Robinson B, Conteduca V, Augello MA, et al. N-Myc-mediated epigenetic reprogramming drives lineage plasticity in advanced prostate cancer. J Clin Invest. 2019; 129: 3924-40.
35. Zhou X, Benson KF, Ashar HR, Chada K. Mutation responsible for the mouse pygmy phenotype in the developmentally regulated factor HMGI-C. Nature. 1995; 376: 771-4.
36. Pentimalli F, Dentice M, Fedele M, Pierantoni GM, Cito L, Pallante P, et al. Suppression of HMGA2 protein synthesis could be a tool for the therapy of well differentiated liposarcomas overexpressing HMGA2. Cancer Res. 2003; 63: 7423-7.
37. Qin XY, Suzuki H, Honda M, Okada H, Kaneko S, Inoue I, et al. Prevention of hepatocellular carcinoma by targeting MYCN-positive liver cancer stem cells with acyclic retinoid. Proc Natl Acad Sci USA. 2017; 115: 4969-74.
38. Vallet-Pichard A, Mallet V, Nalpas B, Verkarre V, Nalpas A, Dhalluin-Venier V, et al. FIB-4: an inexpensive and accurate marker of fibrosis in HCV infection. comparison with liver biopsy and fibrotest. Hepatology. 2007; 46: 32-6.
39. Sterling RK, Lissen E, Clumeck N, Sola R, Correa MC, Montaner J, et al. Development of a simple noninvasive index to predict significant fibrosis in patients with HIV/HCV coinfection. Hepatology. 2006; 43: 1317-25.
40. Clavien PA, Barkun J, de Oliveira ML, Vauthey JN, Dindo D, Schulick RD, et al. The Clavien-Dindo classification of surgical complications: five-year experience. Ann Surg. 2009; 250: 187-96.
41. Shi J, Lai EC, Li N, Guo WX, Xue J, Lau WY, et al. A new classification for hepatocellular carcinoma with portal vein tumor thrombus. J Hepatobiliary Pancreat Sci. 2011; 18: 74-80.

Cite this article as: Qi L, Xu J, Chen Y, Lu Z, Zhou M, Huang Y, et al. Comprehensive strategies for management of postoperative hyper-progression recurrence (HPR) of hepatocellular carcinoma: a 12-year large sample multi-center study. Cancer Biol Med. 2025; 22: 964-987. doi: 10.20892/j.issn.2095-3941.2024.0514